Check for updates

NIST Internal Report
NIST IR 8437

On the Feasibility of COVID-19 Proximity Detection Using Bluetooth Low Energy Signals

Nader Moayeri
Chang Li
Lu Shi

This publication is available free of charge from:
https://doi.org/10.6028/NIST.IR.8437

NATIONAL INSTITUTE OF STANDARDS AND TECHNOLOGY
U.S. DEPARTMENT OF COMMERCE

NIST Internal Report
NIST IR 8437

On the Feasibility of COVID-19 Proximity Detection Using Bluetooth Low Energy Signals

Nader Moayeri
Chang Li
Lu Shi
Smart Connected Systems Division
Communications Technology Laboratory

This publication is available free of charge from:
https://doi.org/10.6028/NIST.IR.8437

November 2022

U.S. Department of Commerce
Gina M. Raimondo, Secretary

National Institute of Standards and Technology
Laurie E. Locascio, NIST Director and Under Secretary of Commerce for Standards and Technology

NIST IR 8437
November 2022

The research reported in this paper was approved under study number CTL-2020-0209 by RPO.

The National Institute of Standards and Technology Research Protections Office reviewed the protocol for this project and determined it is "not human subjects research" as defined in 15 CFR 27, the Common Rule for the Protection of Human Subjects.

Publication History
Approved by the NIST Editorial Review Board on 2022-09-12

How to cite this NIST Technical Series Publication:
N. Moayeri, C. Li, L. Shi (2022) On the Feasibility of COVID-19 Proximity Detection Using Bluetooth Low Energy Signals. (National Institute of Standards and Technology, Gaithersburg, MD), NIST IR 8437. https://doi.org/10.6028/NIST.IR.8437

NIST Author ORCID iDs
Nader Moayeri: 0000-0003-3897-505X

Contact Information
moayeri@nist.gov

Abstract

The COrona VIrus Disease – 2019 (COVID-19) pandemic has had a profound effect on the entire world. With the onset of the pandemic in 2020, also started various efforts around the world to automate the contact tracing process to increase its efficacy. Most of these efforts and the smartphone apps that were developed used the Bluetooth Low Energy (BLE) Received Signal Strength Indicator (RSSI) to detect proximity between people. This was facilitated by the development of the Google-Apple Exposure Notification (GAEN) system that made it possible for Android phones and iPhones to exchange standardized BLE messages seamlessly so that RSSI could be measured by both types of phones.

In the summer of 2020, we carried out a five-week long BLE RSSI data collection campaign using wearable devices developed at NIST and running on a Raspberry Pi platform. The data collection was comprehensive, because it included a wide variety of operational scenarios including situations where the two devices were not in line-of-site of each other. To the best of our knowledge, there are no publicly reported repositories of BLE RSSI data that includes non-line-of-site (NLOS) scenarios. Such scenarios are important, because they can lead to false alarms in detecting situations where virus transmission between two people is possible.

The paper presents a classical analytical framework for proximity detection in the context of electronic contact tracing for COVID-19. We make a distinction between *instantaneous* and *after the fact* proximity detection. In the former case, the purpose is to instantaneously warn people that they are violating social distancing rules. In the latter case, the purpose is to notify people after the fact that they had a close contact of certain duration with an individual who has tested positive for COVID-19 and was capable of transmitting the virus at the time of the contact. We evaluate the performance of various methods for instantaneous proximity detection. In after the fact proximity detection, we are interested in identifying periods of time where two people were too close to each other with no barriers between them. We propose a method that applies the Viterbi Algorithm to a time series of BLE RSSI data to solve this problem. The method exploits the fact that humans do not move faster than certain speed. In both cases of instantaneous and after the fact proximity detection, we show that methods based on BLE RSSI data leave a lot of room for improvement. Therefore, the problem of proximity detection for electronic contact tracing and blunting the spread of highly infectious diseases is far from solved. We also know that the next pandemic is not a matter of *if* but *when*.

Keywords

Bluetooth Low Energy (BLE); COVID-19; Distance Estimation; Electronic Contact Tracing; Exposure Notification; Infectious Diseases; Pandemics; Path Loss Models; Proximity Detection; Received Signal Strength Indicator (RSSI); Receiver Operating Characteristic (ROC) Curve; Smartphones; Viterbi Algorithm; Wearable Devices.

Table of Contents

List of Tables

List of Figures

1. Introduction

Pandemics have plagued humankind since time immemorial. Contact tracing has been identified as an effective means of blunting the spread of pandemics since the eighteenth century [1]. Manual contact tracing is labor-intensive and slow, because a health worker has to conduct an interview with anyone who has contracted the infectious disease and then reach out to all those who have come into contact with the infected person. It is also unreliable, because it relies on the infected person remembering all his/her contacts and the severity of each contact over the incubation period of the disease. In addition, the infected person may not know the names of all the people whom he/she has been in contact with. In 2020, it was reported that newly hired contact tracers in New York City had difficulty finding people who had been exposed to the Severe Acute Respiratory Syndrome CoronaVirus 2 (SARS-CoV-2) [2]. Time is of essence in bringing highly infectious diseases, such as COrona VIrus Disease – 2019 (COVID-19), under control. If it takes more than a few hours to reach out to a person who has been exposed to the virus but might be asymptomatic or presymptomatic, that person may go on infecting other people.

Electronic contact tracing has been introduced to mitigate these problems. In some countries, the movements of people that own smartphones are tracked and recorded around the clock. Contacts between two individuals are detected based on their trajectories as a function of time. Such a solution for electronic contact tracing would be an invasion of people's privacy. This document focuses on a solution where a contact is detected based on the distance between two people without tracking their geolocations. That would be a lesser invasion of privacy.

Electronic contact tracing based on peer-to-peer ranging uses smartphones or wearable devices, such as pendants or wrist bands, to detect "close contacts". The people using these devices can then check the contact information recorded on their devices against the data on a national or regional database of infected individuals to find out if they have been exposed to the virus. There are several factors that determine whether electronic contact tracing can be effective in blunting the spread of infectious diseases. One factor is whether a device can accurately detect close or medically-significant contacts with other devices. The US Centers for Disease Control and Prevention (CDC) has updated its definition of a COVID-19 close contact a few times as more has been learned about how the virus gets transmitted from one person to another. The latest one, as of the time of writing of this report, defines a close contact as "someone who was within 6 feet of an infected person for a cumulative total of 15 minutes or more over a 24-hour period starting from 2 days before illness onset (or, for asymptomatic patients, 2 days prior to test specimen collection) until the time the patient is isolated. The World Health Organization (WHO) additionally includes persons with direct physical contact with a probable or confirmed case, direct care for a patient with probable or confirmed COVID-19 disease without using proper personal protective equipment, and other situations as indicated by local risk assessments [3]." Implicit in this definition is the assumption that there is no barrier between the two individuals involved.

For example, if the individuals are on opposite sides of a wall, there is no possibility of virus transmission. Imagine how hard it would be for a person to keep track of 2-3 minute long encounters with other people over a 24-hour period while also worrying about how far apart they were during each such encounter! It would be simply impractical unless each person carries a little notebook to record the duration of each contact and the separation from each person they run into. Electronic contact tracing automates that process and removes a major burden on people regarding their contacts. Other countries use different but similar looking definitions for a close contact.

Another factor is the adoption rate of electronic contact tracing in the society. That rate has to be high. Aside from social distancing and use of masks, a large percentage of the population has to use electronic contact tracing devices, frequently check whether they have been exposed to the virus by running the contact data recorded on their devices against the database of infected individuals, immediately go into quarantine or get tested for the virus if the system notifies them that they may have been exposed, and ensure that their device identifying profile is uploaded onto the database if they test positive for the virus. A third factor that has a bearing on the adoption rate is whether the electronic contact tracing system, as a whole, is privacy preserving. People need assurances that their health data is not used against them, such as how an employer might treat (potential) employees who have contracted the disease. Another issue that discourages people from using contact tracing devices and apps is that they typically do not like to get a notification that they have to go into quarantine, which is a major inconvenience. A significant portion of the population may put their short-term self-interest ahead of societal interest. The same issue comes up when a person who has tested positive for the virus is supposed to enter his/her device profile into the database of infected individuals. There may not be a great incentive for the person to do so. A thorough understanding of all the factors that affect adoption rate and fully compliant use of electronic contact tracing is beyond the scope of this paper. This paper deals with the first factor only, i.e. whether electronic contact tracing devices are capable of accurately detecting close contacts. This is also called proximity detection.

A number of technologies and methods can be used by a smartphone to estimate the range (distance) to another smartphone. In case of wearable devices, there is a greater variety of technologies and methods for ranging that could be used, because one is not restricted to what is typically available on a smartphone. The simplest solution for ranging is to use the strength of the Bluetooth Low Energy (BLE) signal that a smartphone receives from another one. BLE technology is readily available in all smartphones. The techniques for estimating range based on the received BLE signal is essentially the same whether a smartphone or a wearable device is used. However, there might be some differences depending on which manufacturer's BLE chipset is used in a smartphone or a wearable device.

Google and Apple developed the Exposure Notification (GAEN) System [4] based on Bluetooth technology in 2020. They chose to work with Bluetooth because it is readily available on smartphones. There are currently about 7.26 billion smartphones in use around the world, which has a population of 7.94 billion. Google and Apple developed Application

Programming Interfaces (APIs) to enable Android phones and iPhones to exchange standardized BLE messages. This allows a phone to estimate proximity to other phones based on BLE Received Signal Strength Indicator (RSSI). The phones can also measure the time duration of each encounter or any sub-interval thereof. An encounter is defined as the time interval where the BLE devices "see" each other. That is, each device can correctly receive advertisements from the other device including the ID for that device. According to one website [5], within one year of GAEN's introduction, 26 US states and territories and 39 countries around the world were using the GAEN System. Even though GAEN was designed for use on smartphones, it can also be used on personal wearable electronic devices. GAEN fueled the use of smartphone apps for exposure notification. For our purposes of determining the effectiveness of proximity detection based on BLE RSSI, it does not matter whether the GAEN protocols are implemented on smartphones or personal wearable devices. As a matter of fact, it does not even matter if these protocols are implemented exactly according to the GAEN Bluetooth specification. Google and Apple have suggested the use of a slow rate for exchange of GAEN BLE messages so that the smartphone battery is not depleted quickly. However, one cannot estimate the distance between two devices with adequate time resolution if one uses a low message exchange rate. Making the device battery last longer before it has to be recharged should not come at the expense of not doing as effective a job of blunting the spread of the infectious disease as possible. For these reasons, in this paper we are interested in determining how well proximity detection based on BLE RSSI can be done regardless of how often the smartphone or the personal wearable device has to be charged.

This paper takes an empirical approach to evaluate the performance of various proximity detection schemes based on BLE RSSI. We carried out a comprehensive, five-week long data collection campaign at the NIST Campus in Gaithersburg, Maryland, where we collected BLE RSSI samples recorded by two wearable devices over a large number of radio frequency (RF) signal propagation scenarios. Each scenario lasted about six minutes, with Device 1 transmitting BLE advertisements and Device 2 receiving them in the first three minutes and then switching roles and Device 2 transmitting and Device 1 receiving in the next three minutes. We carefully documented the circumstances under which each data collection scenario was carried out. The parameters that characterize the circumstances under which the BLE RSSI data was collected are called metadata. In each scenario, the two devices involved were mounted on tripods (one device per tripod) and hence were stationary. We measured and documented the distance between the devices.

We study the relationship between BLE RSSI and inter-device distance under different circumstances. The devices can be in line-of-site (LOS) or non-LOS (NLOS) of each other. The latter includes the possibility of a wall or a person being on the straight line from one device to the other. The orientations of the devices with respect to each other affect RSSI. It is one thing to estimate the inter-device distance based on a single or a few RSSI samples and another to detect a close contact as defined by the CDC. The former is useful as a preventive measure to warn people *instantaneously* when they are getting too close to each other. The latter is useful for electronic contact tracing purposes and to notify people *after the fact* that they may have been exposed to the virus. If the system can do a good job on the former, people can try to maintain social distancing whenever possible, and there will be less need for the latter. Unfortunately, as it turns out later in this paper, it is difficult to do a good job on the former based on BLE RSSI. We show a few ways of specifying a function that estimates distance based on a single or a few RSSI samples. As for close contact detection, recall that a close contact may be made of several "mini-contacts" whose durations add up to at least 15 minutes. Therefore, the device has to examine a sequence of RSSI samples several minutes long and look for mini-contacts.

The rest of this paper is organized as follows. Section 2 describes our data collection campaign in detail. In Sec. 3, we study the relationship between BLE RSSI and inter-device distance under various scenarios. Section 4 proposes two ways of estimating inter-device distance based on a single or a few BLE RSSI samples using the classical power-law path loss model. Section 5 deals with the use of the Receiver Operating Characteristic (ROC) curve to characterize the performance of a decision rule on whether two people/devices are in close proximity of each other at a given time instance. It also looks at the M out of N detector as a solution for this problem. Section 6 deals with mini-contact detection, which is a prerequisite for close contact detection. A method based on the Viterbi Algorithm is proposed and its performance evaluated. Section 7 is an overview of related work. Section 8 presents the conclusions of this study and suggests future directions for research.

2. BLE RSSI Data Collection Campaign

Instead of using smartphones for data collection, we developed our own wearable devices based on the Raspberry Pi platform. Specifically, each wearable was a Raspberry Pi Zero W device that could operate either in Tx (transmit) or Rx (receive) mode. In the Tx mode, the device would announce its presence by going through roughly 100 cycles of transmitting advertisements over a three-minute period. In the Rx mode, the device would listen for and record advertisements from the other device for three minutes. In each data collection scenario, we set one device to Tx mode and the other one to Rx mode for three minutes, and then we changed the roles of the two devices for the next three minutes. There are a number of commercially available electronic contact tracing systems that use wearable devices instead of smartphones. There are several reasons why the use of stand-alone wearable devices may be preferable to the use of smartphones. First, not everyone has a smartphone [6]. Second, people may have a lot of personal data on their phones and hence may be reluctant to install an exposure notification app that interacts with public health authorities [7]. They may be concerned about unauthorized use of the data on their phones. Third, interacting with a smartphone may be a barrier to certain segments of the society, such as the elderly [8]. Finally, small children under 10 may not have a smartphone [9] or be capable of being responsible for one. However, from the point of view of how BLE RSSI behaves stochastically, it does not matter whether one uses smartphones or wearable devices for data collection. The only exception might be the differences in the antenna characteristics and beam patterns of the two platforms.

A mini-contact for the purposes of this paper is a maximal-length sub-interval $[t_1, t_2]$ of an encounter between two people, such that the distance between them is less than or equal to six feet during $[t_1, t_2]$ and larger than six feet just before t_1 and just after t_2. Whether a mini-contact should be taken into account towards the formation of a close contact, per CDC definition, is determined when one of the two people involved checks the data collected by his/her device against the database of infected individuals and finds out that the other person was capable of transmitting the virus at the time the mini-contact was made. Note that a BLE device running the GAEN Bluetooth Specification may fail to detect the occurrence of a mini-contact. This is called a missed detection or false negative. Similarly, the BLE device may decide that a mini-contact was made, while in reality it did not occur. This is called a false alarm or false positive. Even if the BLE device correctly detects the occurrence of a mini-contact, its estimates of the beginning or ending times of the mini-contact may not be accurate. (Note that any event in a BLE device has a UNIX timestamp, which has a time resolution of one millisecond.) Therefore, two performance metrics are used to quantify the effectiveness of an electronic contact tracing system in detecting close contacts. One is the false negative rate and the other is the false positive rate. These are indeed conditional probabilities. Also, note that two components determine the performance of a BLE-based electronic contact tracing system. One is the protocol used for exchange of BLE messages, and the other is the algorithm that detects mini-contacts.

In our data collection campaign, we aimed to collect as many BLE RSSI samples as possible over a fixed amount of time in scenarios involving two stationary devices. We let one device transmit advertisements as quickly as possible to announce its presence to the other device for a period of three minutes. Then we switched the roles of the devices and let the second device transmit advertisements while the first one received them. The main goal was to study the relationship between BLE RSSI and the distance between devices.

Based on the definition given earlier, an encounter is a maximal-length subsequence of (timestamp, ID, RSSI) triplets with the same ID, and the time duration of the encounter is the difference between the timestamps of the first triplet and the last one. (Note that the time elapsed from one timestamp to the next one is not necessarily a fixed number.) The part that is challenging is the estimation of the distance between devices at the timestamps associated with the encounter. If the distance can be estimated accurately, which is a big if, and all the distances corresponding to timestamps associated with the i'th through j'th triplets (with $j > i$) are less than or equal to six feet and the distances corresponding to timestamps associated with the $i-1$'st and $j+1$'st triplets are larger than six feet, then we can say that a mini-contact with duration equal to the difference between the timestamps associated with the j'th and i'th triplets has occurred. Therefore, one way to solve the problem of detecting mini-contacts is to find a mapping from a time series of RSSIs, with corresponding timestamps, to a time series of distances with the same timestamps. In practice, and as it will be shown later in this paper, it is not possible to accurately estimate distances from RSSI samples. Hence, there are contact detection algorithms that directly go from a sequence of triplets, as described above, to triplets i and j that mark the beginning and the end, respectively, of a mini-contact. In other words, these algorithms do not try to explicitly estimate the distance between the two devices at each timestamp. Given that inter-device distances cannot be estimated accurately, there is bound to be errors in estimating the times that a mini-contact begins and ends. Note that distance estimation is by far more challenging than determining the starting and ending times of an encounter or mini-contact.

In order to design ranging techniques based on received BLE signal, one has to collect BLE RSSI data under different circumstances and carefully document what those circumstances were. For example, one has to vary the distance between two devices, and collect data when the devices are in LOS or NLOS of each other. The variables that characterize the circumstances under which the BLE RSSI data was collected are called metadata. This section is a recipe for BLE RSSI data collection.

2.1. Important Considerations

A fair amount of planning has to be done before a data collection campaign of the magnitude undertaken in this work can begin. The following is a list of considerations that have to be made:

- Throughout this document, we often talk about "data collection scenarios" or simply "scenarios". Each scenario involves two devices, each mounted on a tripod of its own and kept stationary during data collection. In addition, each device will have its own pose that does not change during data collection. Other "factors" include whether there is an object (wall, person, furniture, etc.) on the direct propagation path (i.e., the straight line from one device to the other) or not. These are called NLOS and LOS signal propagation scenarios, respectively. If there are any object(s) on the direct propagation path, they also remain stationary during data collection.
- In general, the "metadata" related to each scenario needs to be documented in order to make the data useful to other people wishing to use it in their research or repeat our data collection scenarios. We have done our best to document all factors related to each scenario, as described in Subsec. 2.2.
- In each scenario, each device is mounted on a tripod dedicated to that device at a pose specified for that device. This excludes the possibility of a device being in the front or back pocket of someone's pants or being carried in a purse, and whether the person wearing a device is standing or sitting during data collection. It would be easier to measure the distance between any pair of tripods using an accurate laser ranger in LOS scenarios. If such a device is not available, a simple tape measure can be used. Distance measurement in NLOS scenarios will be much harder. When possible, we took advantage of the special markers deployed on the floors in six buildings on the Gaithersburg Campus of NIST to help find the distance between the tripods in NLOS

scenarios. The 3D coordinates of these markers have been professionally surveyed. They are used for test and evaluation of indoor localization systems at NIST.

- In each scenarios, regardless of whether the devices were in LOS or NLOS of each other, we did not follow the GAEN protocol. We let one device transmit advertisements back to back as quickly as possible for three minutes while the other device was in listening / scanning mode. The BLE RSSI data at the second device was recorded. Then we switched device roles and let the second device transmit advertisements for three minutes while the first one listened and its BLE RSSI data was recorded. Typically, the receiving device was able to receive more than 100 advertisements over three minutes of data collection. In some scenarios where the devices could hardly receive signals from each other, the number of advertisements received in three minutes was less than 100. The entire scenario took six minutes to do.
- In some LOS scenarios, a person may be situated on the direct path between the devices. This allowed us to measure how much the RF signal is attenuated by a human body. This scenario arises when a person without a BLE device comes between two people with such devices. In addition, it may approximate the following situations: (i) One device is in the back pocket of a person, the other device is in the front pocket of a second person, and the two people are either facing each other (and possibly talking) or walking away from each other. (ii) Two people are in a line waiting to get into a grocery store, for example, and each has a device in his/her front pocket. It is also possible to mount devices on various locations on phantoms or mannequins instead of mounting them on tripods or let a phantom or mannequin be placed between two devices. We did not use phantoms or mannequins in this study.
- In each scenario, we collected data for various orientations, also called poses, of the devices involved. We were limited in the number of choices for orientation, because otherwise it would have taken forever to carry out the data collection campaign.
- Each wearable device would have a local coordinate system defined in the same way such coordinate systems are defined for smartphones. Figure 1 shows the standard way of defining the local coordinate system for a smartphone.
- We need to define a reference coordinate system, also called the reference frame. We can let Device 1 be the origin of the reference coordinate system, the x-axis be in the direction of the horizontal line connecting Device 1 to the horizontal location of Device 2 (we say horizontal location, because the devices may be at different heights), the z-axis be perpendicular to and pointing away from the floor/ground, and the y-axis be in the horizontal plane containing the x-axis such that the right hand rule applies to the coordinate system. Alternatively, we can let the x-axis point to geographic east, the y-axis point to geographic north, and the z-axis be perpendicular to the ground/floor and pointing away from it. Still, the origin of the coordinate system would be Device 1.

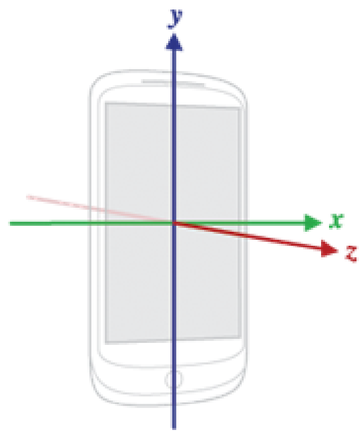

Fig. 1. The local coordinate system for a smartphone

- We need to define the pose of each device with respect to the reference coordinate system. It takes three angles to specify each pose unambiguously, and there are standard ways for doing this.
- There are infinite number of possibilities for the pose of each device, but we can only look at a small number of combinations of poses for the devices involved in a scenario. As described at the beginning of Appendix A, we considered only two combinations of poses for the devices. In our data collection scenarios, either the devices were facing each other or they were both facing up. The devices would face each other when users wear them on their chests like pendants facing forward. In addition, both devices will be placed at 120 cm elevation from the ground/floor.
- One aspect not addressed in our data collection plan is whether the numbers of LOS and NLOS scenarios are proportionate. Unfortunately, it is hard to have a good handle on this issue. One possibility is to argue that the volumes of data we obtain in LOS and NLOS scenarios should be proportionate to their probabilities of occurrence in real life. However, it is not clear how to find those probabilities.

2.2. Metadata and Data File Formats

It is very important to document the metadata associated with each data collection scenario. For example, if two devices are within 1 m of each other but on opposite sides of a wall, then there is no possibility for virus transmission from one person to another. One would know this is the case, if the metadata indicates this was a NLOS scenario with a wall between the two devices. As another example, device poses affect the RSSI at each device. Hence, one may be able to get a more accurate estimate of the range if device poses are known, which may be possible through the use of accelerometer, gyroscope, and magnetometer data readily available in smartphones. These sensors can also be present on a wearable device, even though the ones we used for data collection did not have them.

For each data collection scenario. we stored the following metadata in the same file as the data itself.

- LOS/NLOS
- Scenario ID
- Whether a person was on the direct path between devices
- If a person was on the direct path, whether this person was in the middle of the path or at 50 cm distance from one device
- Device orientations: We collected data using two arrangements only. In one arrangement, the devices faced each other. In the other one, both devices faced up.
- Inter-device distance. This is the distance in 3D and not the horizontal distance. This was needed because the devices were on different floors of a building in one scenario.
- Device models
- For the scenarios involving corners, the construction material of the corner and the 2D locations of Device 1, Device 2, and the corner.
- For the scenarios where the devices were on different floors of a building, the height of each floor and the number of floors between the devices
- For the scenarios where there were walls/objects between the devices, the number of walls/objects and the construction materials of the walls/objects. (Note that the object may be a door or an office partition panel.)
- Transmit power of each BLE device

In each data set, each row comprises the following information:

- Unix time (in milliseconds) for the BLE RSSI sample
- Transmitting device ID
- BLE RSSI sample
- The channel number (37, 38, or 39) on which the BLE signal was received

2.3. Scenarios

The scenarios we used for data collection are catalogued in Appendix A. To the best of our knowledge, this is the largest publicly available set of annotated BLE RSSI data. All the data we collected is available to the public at [10].

3. Relationship between BLE RSSI and Distance

The results presented in this section are based on an analysis of the data from the scenarios described in Appendix A. Table 1 shows the numbers of data samples obtained in different categories of scenarios. Note that only in LOS scenarios we considered placing a person between the devices. Hence, the sum of the last two entries in the table equals 83,024, which is the number of samples from LOS scenarios.

Table 1. Number of BLE RSSI samples by category

Total Number of RSSI Samples	**144,581**
Number of RSSI Samples from LOS Scenarios	83,024
Number of RSSI Samples from NLOS Scenarios	61,557
Number of RSSI Samples from Device 1	71,672
Number of RSSI Samples from Device 2	72,909
Number of RSSI Samples from Scenarios Using Orientation 1	94,845
Number of RSSI Samples from Scenarios Using Orientation 2	49,736
Number of RSSI Samples from Scenarios with No Person Between Devices	42,660
Number of RSSI Samples from Scenarios with a Person Between Devices	40,364

3.1. Effects of Various Factors on RSSI

Our first observation is that on the average Device 2 recorded a higher RSSI than Device 1. Recall that in each scenario we first let Device 2 record RSSI of the BLE signal received from Device 1 for three minutes. Then we let Device 1 record RSSI of the BLE signal received from Device 2 for another three minutes. We take the average of the RSSIs measured by Device 2 and also the average of the RSSIs measured by Device 1. We compute the difference of these averages. Hence, there is one average RSSI difference for each scenario.

In Fig. 2 we have plotted a histogram of the average RSSI differences over all scenarios. As can be seen, the histogram can be well approximated by a bell-shaped curve, but the curve is not centered at 0 dB. The mean difference is 3 dB, the median is 3.1 dB, and the standard deviation is 1.54 dB. The difference is due to imperfections in the manufacturing process. Even though the BLE radio module in these Raspberry Pi devices are manufactured according to the same specifications, the radios in different devices are never going to behave identically.

As mentioned earlier in this report, we studied only two combinations of orientations for the pair of devices. Let O_1 and O_2, respectively, denote the situation where the devices are facing each other and the situation where both devices are facing up. We look at the RSSI difference between the two orientations over all scenarios. Figure 3 shows that the RSSI is 9.96 dB larger when we compare O_1 against O_2. In addition, the median for the difference is 9.88 dB and the standard deviation is 6.68 dB.

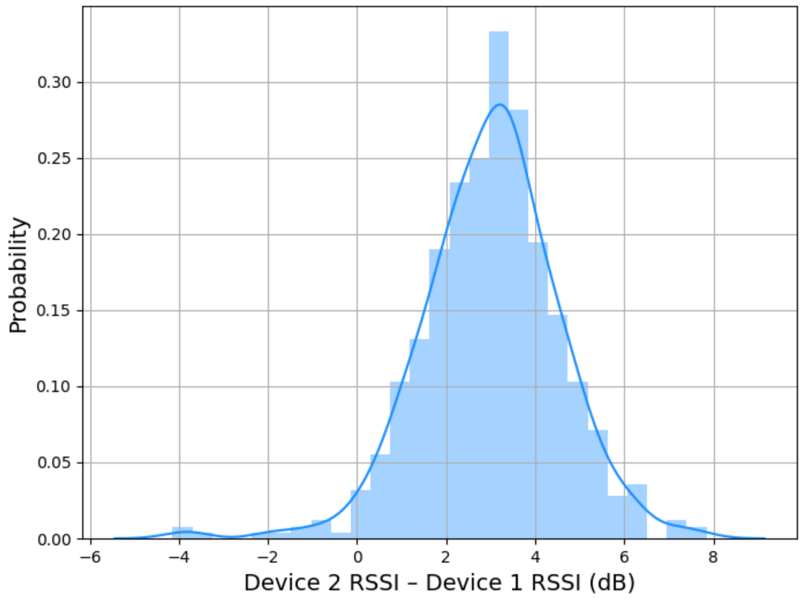

Fig. 2. Histogram of RSSI difference between Device 2 and Device 1

This difference is due to the antenna beam patterns on these devices. The antennas are not omni-directional. The transmitted signal is strongest along certain direction. Similarly, the antenna has a larger sensitivity along certain directions for receiving signals.

We expect the presence of a person on the direct path from one device to another cause an attenuation of the received signal. This attenuation is larger when the person is close to one of the devices as opposed to being for example at the midpoint of the direct path. Figure 4 shows the histogram of the RSSI difference when no one blocks the direct path and when a person is on the direct path at 50 cm distance from one of the devices. Hence, the person is close to the transmitting device for half the duration of a scenario and close to the receiving device for the other half. The figure shows that, on the average, the RSSI is attenuated by about 11.55 dB as a result of the person blocking the direct path. In addition, the median of the RSSI difference is 11.04 dB and its standard deviation is 5.52 dB.

3.2. Effect of Construction Material on Signal Attenuation

In this subsection, we study the extent by which six types of walls attenuate the BLE signal. We kept the transmit power of a pair of BLE devices fixed at a given level. Hence, a lower RSSI indicates higher attenuation. We placed the devices 1 meter apart with a wall between them in the middle. Table 2 shows the mean RSSI for each of four possible device/orientation combinations. We did not make any attempt to compute the path loss for each type of wall. However, if one computes the average of the numbers on each row

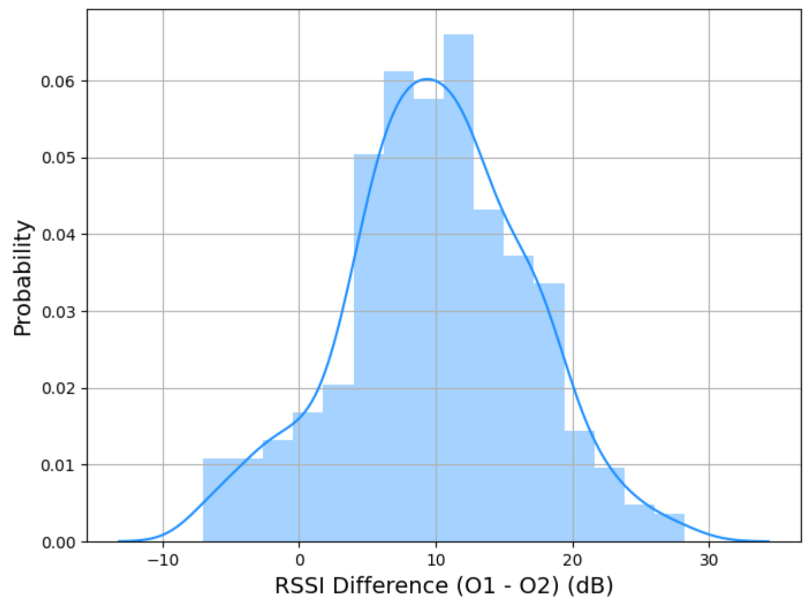

Fig. 3. Histogram of RSSI difference between Orientation 1 and Orientation 2

of the table, one gets an idea how much each type of wall attenuates the signal. In fact, the six wall types have been placed in the table in the order of increasing attenuation and hence decreasing mean RSSI. It has to be noted that the dry wall had metal studs. We observe a 20 dB gap in path loss between the glass wall and the metal wall. In short, the wall type has a substantial effect on the extent of BLE signal attenuation.

4. Analysis

In this section we present a model for BLE RSSI data and methods for estimating the range between two devices based on that model. We also delve into the classification problem of deciding whether two BLE devices are in proximity of each other or not.

4.1. Path Loss Model

The classical model for characterizing the power P_R (in dB) received by a radio is the power law path loss model [11] given by

$$P_R = P_0 - 10\alpha \log_{10} R + X \quad , \tag{1}$$

where R is the distance between the transmitting and receiving radios, P_0 is the received power P_R at $R = 1$, α is the path loss model exponent, and X is a zero-mean Gaussian

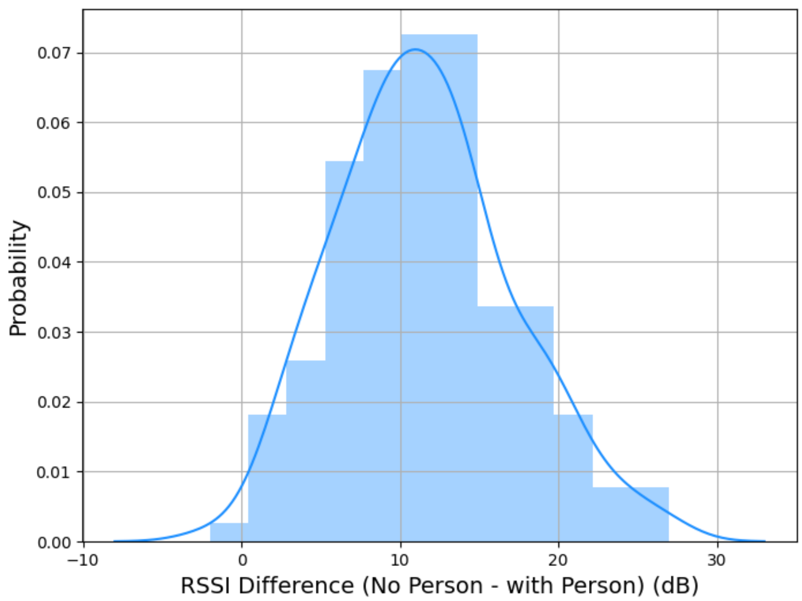

Fig. 4. Histogram of RSSI difference between the case where no one was blocking the direct path and the case where a person was on the direct path at 50 cm distance from one of the devices

random variable with variance σ^2 modelling log-normal fading.

Typically, a least squares method is used to fit a straight line to a scatter plot of P_R vs. $\log_{10} R$ obtained from empirical data. Then α would be the absolute value of the slope of the best-fit line and σ^2 would be the mean squared error of the fit. We applied this method to the scatter plot of BLE RSSI vs. $\log_{10} r$ for all the $144,581$ BLE RSSI samples we collected, as shown in Fig. 5. The parameters for the model are $\alpha = 1.3$ and $\sigma^2 = 129.15$. All the plots presented in this section are based on these values of α and σ^2. One may wonder why the scatter plot looks like a set of vertical bars as opposed to a point cloud. The reason is that we used a discrete set of distances for data collection, like 0.5 m, 1 m, 2 m, etc.

In addition to using the above method on the entire set of collected data, some papers also present the results of applying the same method to the LOS and NLOS data separately. In other words, they obtain a power law path loss model for LOS signal propagation scenarios and another one for NLOS scenarios. Even though this is straightforward, we have not done it because in reality when two people with wearable BLE devices are in proximity of each other, there is no way for the devices to determine whether they are in LOS or NLOS of each other.

We have already mentioned that GAEN notifies people *after the fact* that they have had close contact with someone who has tested positive for the virus. That approach basically

Table 2. Mean BLE RSSI with the signal propagated through different type of walls (unit: dBm)

	Device 1 Orientation 1	Device 2 Orientation 1	Device 1 Orientation 2	Device 2 Orientation 2
Glass	-31	-29	-37	-32
Cinder Block	-32	-30	-37	-34
Brick	-30	-28	-39	-39
Dry Wall	-41	-40	-45	-42
Granite	-52	-52	-46	-42
Metal	-57	-54	-52	-49

mimics conventional contact tracing. An alternative method to blunt the spread of COVID-19 or other highly infectious diseases is to warn people *"(near-)instantaneously"* that they are getting too close to another person and are about to violate social distancing guidelines. For example, the wearable device can start beeping softly and/or vibrate. We say near-instantaneously, because the warning does not have to be issued as soon as the device sees an RSSI sample larger than some threshold. For example, if the RSSI is being sampled at a 10 Hz rate, there is no problem if the wearable device observes 10 additional samples after the first sample that might indicate that the distance has dropped below six feet. This is OK, because it is very unlikely that the virus would get transmitted in one second.

A simple method for estimating the distance between two wearable BLE devices is to plug the measured RSSI in the equation for the best fit line, which is essentially Eq. (1) without the X term, and solve for R. Therefore, in principle, one can obtain an estimate of the inter-device distance for each RSSI sample and use this information for detecting mini-contacts by looking for runs of range estimates $\leq$ six feet. However, this method is not going to be effective, because the relationship between RSSI and range is far from being deterministic due to the large variance of log-normal fading X. A more effective method for detecting mini-contacts is presented in Sec. 6.

In the rest of this section, we present some properties of the power law path loss model and their implications through basic analysis.

4.2. Estimator Bias and Mean Squared Error

Consider a time series of BLE RSSI samples modelled according to the path loss model given in Eq. (1):

$$P_{R,i} = P_0 - 10\alpha \log_{10} R + X_i \quad ; \quad i = 1, 2, \ldots, N \tag{2}$$

where we have assumed that the range R remains constant over the N observations and X_1, X_2, ..., X_N are i.i.d. Gaussian random variables with zero mean and variance σ^2. R would

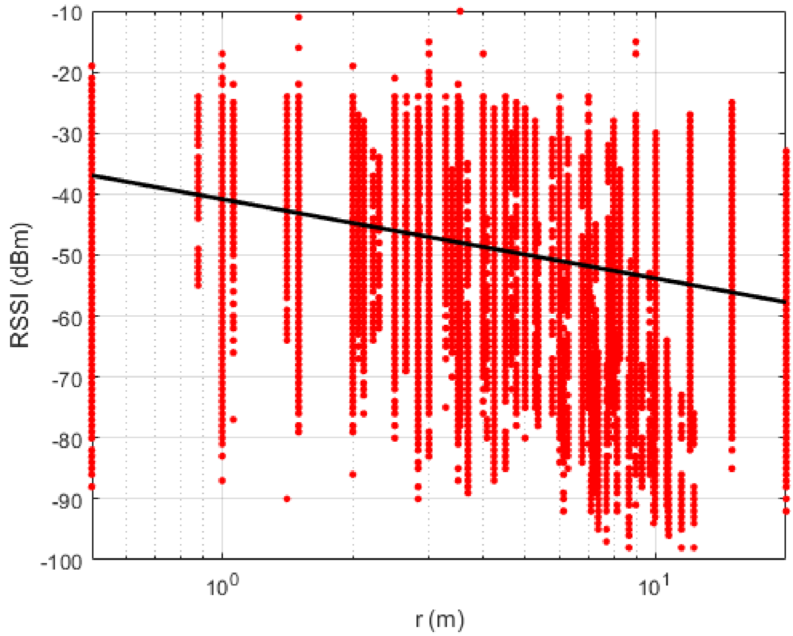

Fig. 5. Power law path loss model for BLE RSSI data

remain constant if the people with wearable devices are not moving, for example, or when the RSSI sampling rate is fast enough that there is little change in the inter-device distance R over N observations. These assumptions are not needed in the $N = 1$ special case.

By the law of large numbers, $\frac{1}{N}\sum_{i=1}^{N} P_{R,i}$ converges to $P_0 - 10\alpha\log_{10} R$. Therefore, the following would be a reasonable estimate for R based on observations $P_{R,1}, P_{R,2}, \ldots, P_{R,N}$:

$$\hat{R}_N = 10^{\left[P_0 - \frac{1}{N}\sum_{i=1}^{N} P_{R,i}\right]/(10\alpha)} \tag{3}$$

It is straightforward to show that

$$E\left[\hat{R}_N | R = r\right] = re^{\frac{\sigma^2 \ln^2 10}{200\alpha^2 N}} = rK_N \quad , \tag{4}$$

where we have introduced

$$K_N = e^{\frac{\sigma^2 \ln^2 10}{200\alpha^2 N}} \tag{5}$$

It is clear that $\hat{R}_N$ is not an unbiased estimate of R based on $P_{R,1}, P_{R,2}, \ldots, P_{R,N}$. However, $\hat{R}_N$ is asymptotically unbiased as $N \to \infty$. The conditional mean squared error (MSE) of $\hat{R}_N$ is

$$E\left[(\hat{R}_N - R)^2 | R = r\right] = r^2\left[1 - 2K_N + K_N^4\right] \quad , \tag{6}$$

which tends to zero as $N \to \infty$, because K_N tends to one as $N \to \infty$. The top curve in Fig. 6 is a plot of the conditional MSE of $\hat{R}_N$ normalized by r^2 as a function of N. The other two curves will be explained in later subsections.

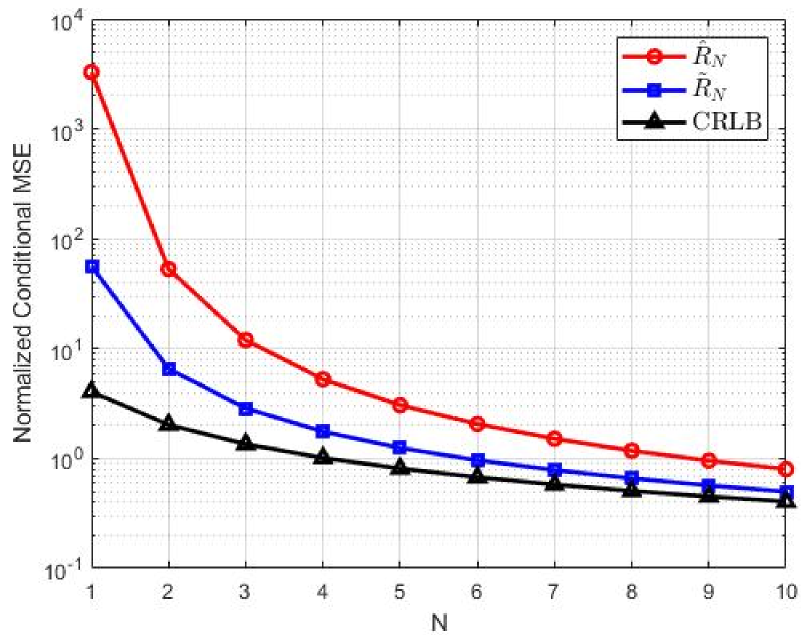

Fig. 6. Normalized conditional MSEs of two estimators and normalized CRLB

4.3. Autocorrelation/Autocovariance

In any detection or estimation problem, the more is known about the random process of observations and how it relates to what has to be detected or estimated, the higher the likelihood of being able to develop a more effective detection/estimation scheme. This principle applies to the proximity detection considered in this paper as well. The observation is the sequence of BLE RSSI measurements made by a wearable device or a subset of that random process. Complete characterization of that random process in the sense of being able to specify the joint probability distribution of any subset of finite size of the RSSI samples is very challenging due to at least two factors. First, the distance between a pair of BLE wearable devices used for proximity detection varies with time. Second, environmental factors affect RSSI measurements. The link between the devices can be LOS or NLOS, and the types of objects found around the devices change over time.

We can, however, look at how any pair of RSSI measurements are correlated to each other. Figure 7 shows the normalized autocovariance of the RSSI random process computed empirically using all 144,581 RSSI samples obtained from all scenarios. In other words, the plot shows the correlation coefficient between pairs of RSSI samples at various time lags. The figure shows that the RSSI random process is for all practical purposes uncorrelated. This is consistent with the power law path loss model presented in Subsec. 4.1 and Subsec. 4.2. Samples of lognormal fading X are i.i.d. Gaussian in that model. Hence, RSSI samples in each scenario are uncorrelated. Note that the mean value for RSSI varies from one scenario to another, because it depends on the distance between the devices. Therefore, we computed the mean RSSI for each scenario separately and subtracted it from the RSSI samples before proceeding with normalized autocovariance computations.

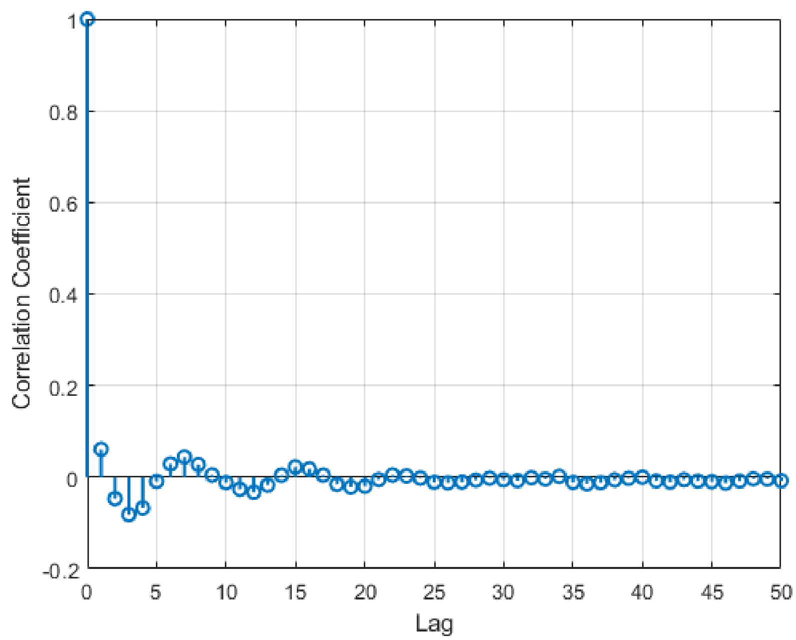

Fig. 7. Normalized autocovariance of the RSSI random process

4.4. Confidence

Consider a binary hypothesis testing problem with hypotheses

- H_1: The pair of devices are ≤ 6 feet apart
- H_0: The pair of devices are > 6 feet apart

and the following decision rule:

$$g(\hat{R}_N) = \begin{cases} H_1 & ; \text{ if } \hat{R}_N \leq 6 \text{ feet} \\ H_0 & ; \text{ if } \hat{R}_N > 6 \text{ feet} \end{cases}$$

In the rest of this paper, we will use 1.83 m instead of 6 feet, even though it makes our equations look awkward! We do this because all our data collection scenarios use meters as the unit for the distance. In addition, the horizontal axis in Fig. 5 is in meters, which affects the value of α.

Su et. al. [12] introduced the notion of confidence as a novel way of assessing the performance of a decision rule for whether the pair of devices are within 1.83 m of each other or not. They define confidence as (Eq. (10d) in [12]):

$$\gamma(r) = \mathrm{P}\left(\left[\hat{R} \leq 6 | P_R \leq P_6\right] \cap \left[\hat{R} > 6 | P_R > P_6\right]\right)$$

where the distances are in feet. This looks like the probability of intersection of two events, but there is a condition associated with each event and the conditioning events are complements of each other. We find this notation confusing. We define $\gamma(r)$ in a different way, but our final result for the $N = 1$ case will be the same as Eq. (10d) in [12].

Let $\hat{\mathrm{C}}$ denote the event that a correct decision is made. We define $\hat{\gamma}(r)$ as

$$\hat{\gamma}(r) = \mathrm{P}(\hat{\mathrm{C}} | R = r) \tag{7}$$

Intuitively, we expect $\hat{\gamma}(r)$ to be large when r is large or when it is close to zero. In addition, we expect it to be small when r is close to 1.83 m. We can write $\hat{\gamma}(r)$ in the following form:

$$\hat{\gamma}(r) = \begin{cases} \mathrm{P}(\hat{R}_N \leq 1.83 | R = r) & ; \quad \text{if } r \leq 1.83 \\ \mathrm{P}(\hat{R}_N > 1.83 | R = r) & ; \quad \text{if } r > 1.83 \end{cases}$$

After a bit of algebra, one can derive the following:

$$\hat{\gamma}(r) = Q\left(\frac{-10\alpha\sqrt{N}}{\sigma}\left|\log_{10}\frac{r}{1.83}\right|\right) = 1 - \frac{1}{2}\mathrm{erfc}\left(\frac{10\alpha}{\sigma}\sqrt{\frac{N}{2}}\left|\log_{10}\frac{r}{1.83}\right|\right) \tag{8}$$

Figure 8 is a plot of $\hat{\gamma}(r)$ for various values of N. It shows that confidence increases with N at *any* r and hence better decisions are made on whether a pair of BLE devices are within 1.83 m of each other or not. Just in case it is not clear, the point where all three curves achieve their minima is at 1.83 m.

4.5. An Unbiased Estimator

We can make $\hat{R}_N$ unbiased by multiplying it by K_N^{-1}:

$$\tilde{R}_N \triangleq K_N^{-1}\hat{R}_N = e^{-\frac{\sigma^2 \ln^2 10}{200\alpha^2 N}}\hat{R}_N \tag{9}$$

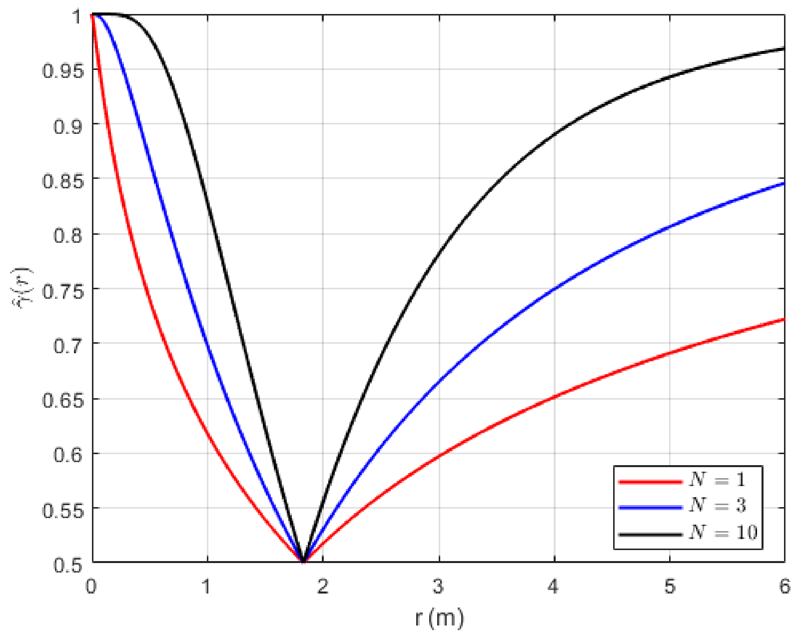

Fig. 8. The confidence function $\hat{\gamma}(r)$ plotted for $N = 1, 3, 10$

It is straightforward to compute the conditional MSE of $\tilde{R}_N$ as

$$E[(\tilde{R}_N - R)^2 | R = r] = \text{var}\left[\tilde{R}_N | R = r\right] = r^2\left[K_N^2 - 1\right] \quad , \tag{10}$$

which also tends to zero as $N \to \infty$. The middle curve in Fig. 6 is a plot of the conditional MSE of $\tilde{R}_N$ normalized by r^2 vs. N. As shown in the figure, $\tilde{R}_N$ has a smaller conditional MSE than $\hat{R}_N$. Mathematically, this is the case because $K_N > 1$ implies

$$K_N^2 - 1 < 1 - 2K_N + K_N^4 \tag{11}$$

Consider using the decision rule introduced in Subsec. 4.4 with $\hat{R}_N$ replaced by $\tilde{R}_N$, i.e.

$$g(\tilde{R}_N) = \begin{cases} \mathrm{H}_1 & ; \quad \text{if } \tilde{R}_N \leq 1.83 \\ \mathrm{H}_0 & ; \quad \text{if } \tilde{R}_N > 1.83 \end{cases}$$

and let $\tilde{\mathrm{C}}$ denote the event that a correct decision is made with this decision rule. We define $\tilde{\gamma}(r)$ as

$$\tilde{\gamma}(r) = \mathrm{P}(\tilde{\mathrm{C}} | R = r) \tag{12}$$

It can be shown that

$$\tilde{\gamma}(r) = \begin{cases} Q\left(\frac{10\alpha\sqrt{N}}{\sigma}\log_{10}\frac{r}{1.83K_N}\right) & ; \text{ if } r \leq 1.83 \\ Q\left(\frac{-10\alpha\sqrt{N}}{\sigma}\log_{10}\frac{r}{1.83K_N}\right) & ; \text{ if } r > 1.83 \end{cases}$$

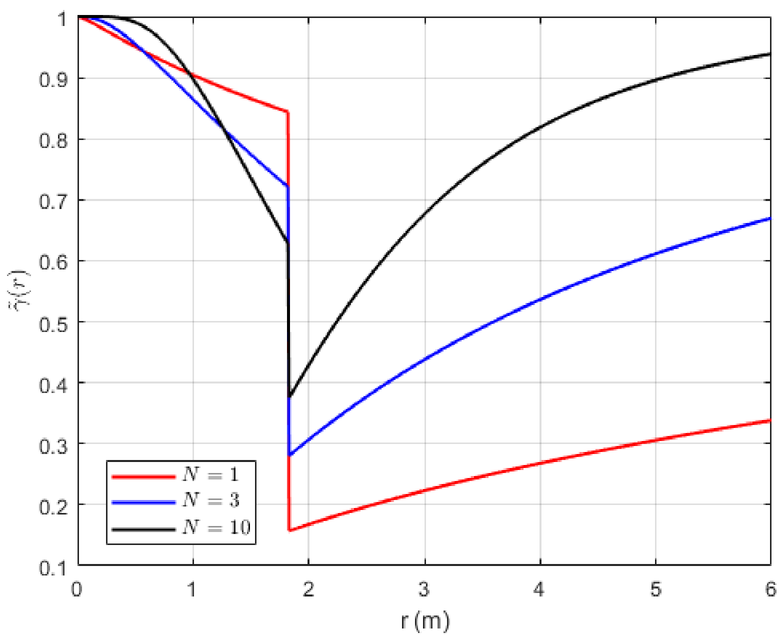

Fig. 9. The confidence function $\tilde{\gamma}(r)$ plotted for $N = 1,3,10$

Figure 9 is a plot of $\tilde{\gamma}(r)$ for various values of N. While $\hat{\gamma}(r)$ is a continuous function, $\tilde{\gamma}(r)$ has a jump discontinuity at $r = 1.83$. In addition, it is no longer true that increasing N results in an increase in confidence at *every* r.

It is easy to show the following

$$\tilde{\gamma}(r) > \hat{\gamma}(r) \quad ; \quad \text{if } r \leq 1.83$$

$$\tilde{\gamma}(r) < \hat{\gamma}(r) \quad ; \quad \text{if } r > 1.83$$

which means that neither $g(\hat{R}_N)$ nor $g(\tilde{R}_N)$ has an advantage over the other in terms of yielding higher confidence. This relationship is shown in Fig. 10 for various values of N.

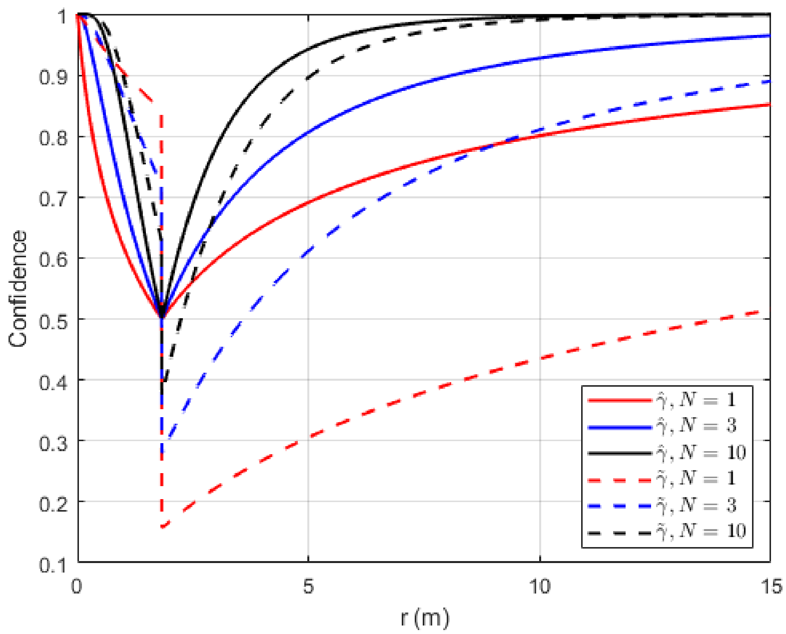

Fig. 10. Comparison of $\hat{\gamma}(r)$ and $\tilde{\gamma}(r)$ for $N = 1, 3, 10$

4.6. Crámer-Rao Lower Bound (CRLB)

The CRLB for *any* unbiased estimate $\check{R}_N$ of R based on observations $P_{R,1}, P_{R,2}, \ldots, P_{R,N}$ has been given in the first line of Eq. (11b) in [12]. We just include it here for the sake of completeness:

$$\operatorname{var}\left(\check{R}_N | R = r\right) \geq \text{CRLB} = \frac{\sigma^2 \ln^2 10}{100\alpha^2 N} r^2 = (2 \ln K_N) r^2 \tag{13}$$

The bottom curve in Fig. 6 is a plot of the CRLB normalized by r^2 as a function of N. As expected, we note that

$$\operatorname{var}\left[\tilde{R}_N | R = r\right] = \left[K_N^2 - 1\right] r^2 \geq \text{CRLB} \quad ,$$

because $K_N > 1$.

5. Classification Performance

The use of confidence for characterizing the performance of a decision rule is an interesting approach, but it is not as common as the use of ROC curve in classification problems. The ROC curve is a plot of detection probability P_{D} vs. false alarm probability P_{FA} for a given decision rule. Different points on the curve correspond to the use of different values for an operational parameter in the decision rule. There would be a family of ROC curves if there are several parameters that can be adjusted.

5.1. ROC Curve

Consider the following decision rule based on observation vector $\underline{P}_R = (P_{R,1}, P_{R,2}, \ldots, P_{R,N})$:

$$h(\underline{P}_R, \delta) = \begin{cases} \mathrm{H}_1 & ; \text{ if } \frac{1}{N}\sum_{i=1}^{N} P_{R,i} \geq \delta \\ \mathrm{H}_0 & ; \text{ otherwise} \end{cases}$$

We note that both $g(\hat{R}_N)$ and $g(\tilde{R}_N)$ that were introduced in Subsec. 4.4 and Subsec. 4.5, respectively, are special cases of $h(\underline{P}_R, \delta)$. We let $p_R(r)$ denote the *a priori* probability density function of R and proceed to compute P_{D} and P_{FA} for $h(\underline{P}_R, \delta)$:

$$\begin{aligned} P_{\mathrm{D}}(\delta) &= \mathrm{P}\left(\frac{1}{N}\sum_{i=1}^{N} P_{R,i} \geq \delta \,\middle|\, R \leq 1.83\right) \\ &= \mathrm{P}\left(P_0 - 10\alpha\log_{10} R + \frac{1}{N}\sum_{i=1}^{N} X_i \geq \delta \,\middle|\, R \leq 1.83\right) \\ &= \frac{1}{\mathrm{P}(R \leq 1.83)}\int_0^{1.83} p_R(r)\mathrm{P}\left(\frac{1}{N}\sum_{i=1}^{N} X_i \geq \delta - P_0 + 10\alpha\log_{10} r\right) dr \\ &= \frac{\int_0^{1.83} p_R(r) Q(\frac{\sqrt{N}}{\sigma}(\delta - P_0 + 10\alpha\log_{10} r))dr}{\int_0^{1.83} p_R(r)dr} \end{aligned}$$

and similarly

$$P_{\mathrm{FA}}(\delta) = \frac{\int_{1.83}^{\infty} p_R(r) Q(\frac{\sqrt{N}}{\sigma}(\delta - P_0 + 10\alpha\log_{10} r))dr}{\int_{1.83}^{\infty} p_R(r)dr}$$

It is clear that both $P_{\mathrm{D}}(\delta)$ and $P_{\mathrm{FA}}(\delta)$ depend on $p_R(r)$. In practice, it is difficult to know $p_R(r)$. One advantage of confidence over the ROC curve is that it does not require the knowledge of $p_R(r)$. The only thing that can be written that somewhat characterizes the relationship between $P_{\mathrm{D}}(\delta)$ and $P_{\mathrm{FA}}(\delta)$ is the following:

$$P_{\mathrm{D}}(\delta)\mathrm{P}(R \leq 1.83) + P_{\mathrm{FA}}(\delta)\mathrm{P}(R > 1.83) = E\left[Q\left(\frac{\sqrt{N}}{\sigma}(\delta - P_0 + 10\alpha\log_{10} R)\right)\right]$$

The hypotheses H_1 and H_0, introduced in Subsec. 4.4, were the basis for developing the notion of confidence and saying something about the ROC curve in this subsection. In reality, one does not care whether a pair of devices are within 1.83 m of each other at a given time instance but rather whether there is potential for virus transmission. For example, there is no possibility of virus transmission if the devices are 1 m apart but on the opposite sides of a wall. Fortunately, it is plausible to assume there is little chance of virus transmission when RSSI values are small. The RSSI is typically small if the pair of devices are in LOS of each other but far apart or when they are in NLOS of each other.

When we talk about the potential for virus transmission in this subsection, we ignore how long a particular situation (the separation between the devices and whether they are in LOS or NLOS of each other) may last. For two reasons, what we have done here is not an exercise in vanity. First, the distance between the pair of devices remained the same during the entire duration of any of our RSSI data collection scenarios. Second, it is acceptable to ignore time duration if the goal is to warn people *instantaneously* that they are getting too close to each other and there is potential for virus transmission as opposed to notifying them about a potential exposure to the virus *after the fact*. Mini-contact detection, which is a prerequisite for exposure notification, is treated in Sec. 6. We show next that there is a way to obtain the ROC curve without the need to explicitly specify $p_R(r)$.

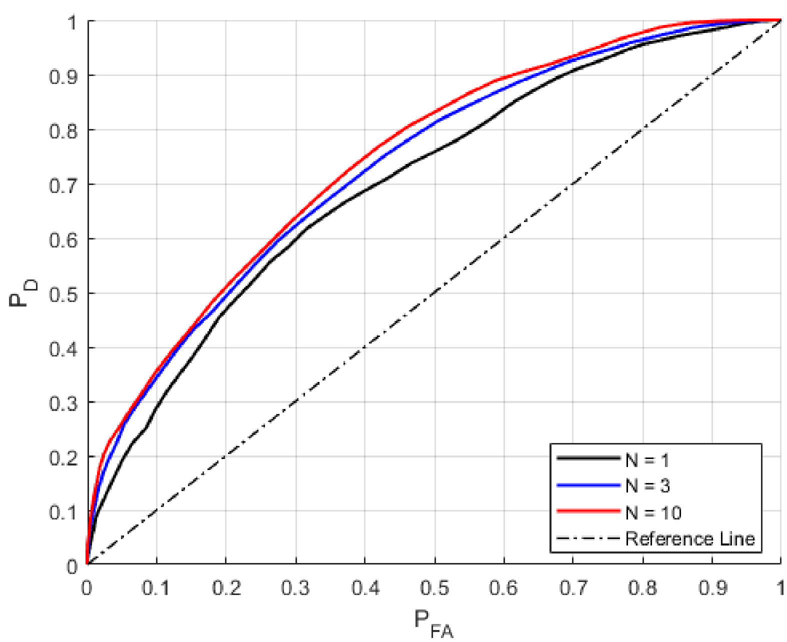

Fig. 11. Mean RSSI Detector with different N

We label any LOS scenario with inter-device distance no larger than 1.83 m as H_1, i.e. there is potential for virus transmission. All other scenarios, namely LOS scenarios with inter-device distance larger than 1.83 m and NLOS scenarios, are labeled as H_0, i.e. there is no potential for virus transmission. We apply $h(\underline{P}_R, \delta)$ to N-blocks of RSSI data obtained from each data collection scenario. We can use non-overlapping blocks or let the blocks have overlap to increase the number of blocks available for analysis and hence obtain more statistically significant results. For each block, the decision rule makes a decision, H_1 or H_0, that can be compared with the ground truth (label of the block). This procedure allows us to compute $P_D(\delta)$ and $P_{FA}(\delta)$ for a given δ.

5.2. M out of N Detector

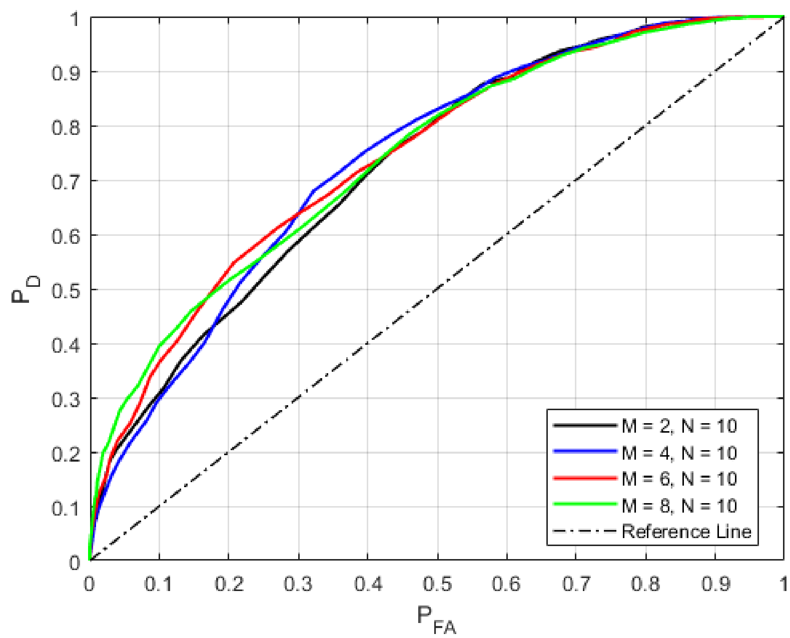

Fig. 12. M out of N detector with different M

The M out of N detector, also called coincidence detector, has long been used by the radar community [13–16]. For $i = 0, 1, \ldots, N-1$, let

$$q_\delta(P_{R,i}) = \begin{cases} 1 & ; \quad \text{if } P_{R,i} \geq \delta \\ 0 & ; \quad \text{otherwise} \end{cases}$$

The detector is then given by

$$\hat{h}(\underline{P}_R, M, N, \delta) = \begin{cases} H_1 & ; \quad \text{if } \sum_{i=1}^{N} q_\delta(P_{R,i}) \geq M \\ H_0 & ; \quad \text{otherwise} \end{cases}$$

Figure 11 shows the ROC curve for the mean RSSI detector for different values of N. This is the detector that was introduced at the beginning of Subsec. 5.1. As N in increased, one sees an improvement in the detector performance although the improvement from $N = 3$ to $N = 10$ is marginal.

Figure 12 shows the ROC curve for the M out of N detector for $N = 10$ and various values of M. The only thing that can be said is that $M = 2$ is not the best choice. The other three values of M are each best in certain range for P_{FA}.

Finally, Fig. 13 is a comparison of the best mean RSSI detector we found with arguably the best M out of N detector. Surprisingly, the mean RSSI detector is better, even though we expected the M out of N detector, due to its nonlinear nature, to be better.

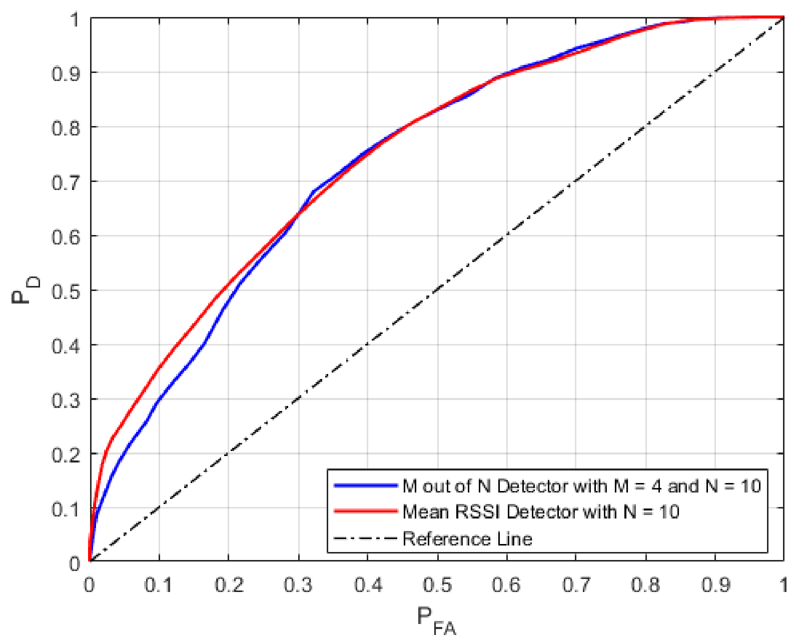

Fig. 13. Comparison of different detectors

6. Mini-Contact Detection

Recall that a mini-contact is a time window of finite, unknown duration during which two people were situated in such a way that there was potential for virus transmission if at least one of them had the virus. In the context of COVID-19, this means the two individuals were in LOS of each other and no more than six feet apart. In this paper, we do not consider other factors, such as ventilation and what kind of activity the individuals were involved in, such as talking or strenuous physical activity. Mini-contact detection, in the context of this paper, is a method for identifying such contacts based on BLE RSSI measurements.

In this section, we present a method for mini-contact detection based on the Viterbi algorithm. The key enabler for this method is a human mobility model that restricts the speed at which a human moves to 1.4 m/s. This is average human walking speed. We do not consider running or any type of motion faster than this. The implication of this model is that the distance between a pair of BLE wearable devices worn by two people cannot change by more than 2.8 m/s. This restriction enables the proposed method to do a better job of estimating the inter-device distance than without using the mobility model.

6.1. A Solution Based on the Viterbi Algorithm

We cast mini-contact detection as a state estimation problem in a stochastic dynamical system and use the Viterbi Algorithm (VA) to solve the problem. The system comprises two people, each wearing a BLE device, the dynamics of their mobility, and the environment as it pertains to RF signal propagation. The state of the system at any given time is a range of values for the distance between the devices and a simple LOS vs. NLOS classification of the signal propagation between them.

Let R denote the distance between the BLE devices and consider a system with state space $\mathscr{S} = \{1, 2, \ldots, 2J\}$ defined below

- j : LOS path, $R \in (\eta_{j-1}, \eta_j]$; $j = 1, 2, \ldots, J-1$
- J : LOS path, $R \in (\eta_{J-1}, \eta_J)$
- $J + j$: NLOS path, $R \in (\eta_{j-1}, \eta_j]$; $j = 1, 2, \ldots, J-1$
- $2J$: NLOS path, $R \in (\eta_{J-1}, \eta_J)$

where $\eta_0 = 0$ and $\eta_J = \infty$. We further assume there exists a positive integers J^* such that $\eta_{J^*} = 1.83$ m. Hence, the possibility of virus transmission exists only in the first J^* states, i.e. $\mathscr{S}^* = \{1, 2, \ldots, J^*\}$.

Let $(p_{R,1}, p_{R,2}, \ldots, p_{R,N})$ be a sequence of negative integers denoting BLE RSSIs measured by one of the BLE devices at times $\underline{t} = (t_1, t_2, \ldots, t_N)$. The reason we have introduced $\underline{t}$ is that the timestamps for RSSI measurements in our prototype system are not equi-spaced. In a prototype with periodic measurements, one would have $t_n - t_{n-1} = T$, for $n = 2, 3, \ldots, N$, for some $T > 0$. Our state estimation problem is to find a sequence of states $\underline{s} = (s_1, s_2, \ldots, s_N) \in \mathscr{S}^N$ that maximizes $\mathrm{P}(\underline{S} = \underline{s} | \underline{P}_R = \underline{p}_R)$ or equivalently

$$\mathrm{P}(\underline{P}_R = \underline{p}_R, \underline{S} = \underline{s}) = \mathrm{P}(S_1 = s_1) \left[\prod_{i=1}^{N} \mathrm{P}(P_{R,i} = p_{R,i} | S_i = s_i) \right] \left[\prod_{j=2}^{N} \mathrm{P}(S_j = s_j | S_{j-1} = s_{j-1}) \right]$$

This is equivalent to finding $\underline{s} \in \mathscr{S}^N$ that minimizes the cost function

$$C(\underline{s}) = -\ln \mathrm{P}(S_1 = s_1) - \sum_{i=1}^{N} \ln \mathrm{P}(P_{R,i} = p_{R,i} | S_i = s_i) - \sum_{j=2}^{N} \ln \mathrm{P}(S_j = s_j | S_{j-1} = s_{j-1}) \quad (14)$$

Let $\underline{\hat{s}}$ be a (or perhaps "the") solution to this minimization problem. A mini-contact is a maximal-length subsequence $(\hat{s}_L, \hat{s}_{L+1}, \ldots, \hat{s}_U)$ of successive samples in $\underline{\hat{s}}$ whose elements are all members of $\mathscr{S}^*$. That is, $(\hat{s}_L, \hat{s}_{L+1}, \ldots, \hat{s}_U)$ has the following properties:

- $\hat{s}_k \in \mathscr{S}^*$, for any $k \in \{L, L+1, \ldots, U\}$.
- If $L > 1$, then $\hat{s}_{L-1} \in \mathscr{S} - \mathscr{S}^*$.
- If $U < N$, then $\hat{s}_{U+1} \in \mathscr{S} - \mathscr{S}^*$.

Note that there may exist several mini-contacts in $\underline{\hat{s}}$. Our methodology attempts to find all of them.

This minimization problem can be efficiently solved using the VA [17], which finds the best path in the N-stage trellis with $2J$ states at each t_j. The set of possible transitions from states at timestamp t_{j-1} to states at timestamp t_j would be the same for each j, if the RSSI measurements are made in a periodic fashion. In the general case, where the timestamps are not equi-spaced, as is the case in our system, the set of possible transitions would depend on $\Delta_j = t_j - t_{j-1}$, for $j = 2, 3, \ldots, J$.

Let's examine how the three terms in the right hand side of Eq. (14) can be computed. The first term is the simplest. For any $s_1 \in \mathscr{S}$, we can estimate $\mathrm{P}(S_1 = s_1)$ from our empirical data. For each data collection scenario, we know the distance between the devices and whether it was a LOS or NLOS scenario. Therefore, each data record (consisting of timestamp, RSSI value, etc.) in a given scenario gets the same label from $\mathscr{S}$. Then for each $s_1 \in \{1, 2, \ldots, J\}$, we count the number of data records labeled s_1. This results in a histogram for LOS scenarios. Similarly, for each $s_1 \in \{J+1, J+2, \ldots, 2J\}$, we count the number of data records labeled s_1. This results in a histogram for NLOS scenarios. For a given set of η_j's and depending on how extensive the data collection was, it may turn out that a few terms in each histogram would be zeroes. This would not be realistic, because it would imply that the distance between the devices cannot fall in certain intervals. To alleviate this problem, we fit a smooth curve to each histogram and sample each curve at $\{(\eta_{j-1} + \eta_j)/2 : j = 1, 2, \ldots, J-1\}$ and at $(3\eta_{J-1} - \eta_{J-2})/2$. Then we normalize each histogram so that the terms in each histogram add up to one. The last step is to combine the two normalized histograms using the total numbers of LOS and NLOS data records to arrive at an estimate for $\mathrm{P}(S_1 = s_1)$ for any $s_1 \in \mathscr{S}$.

The estimates for $\mathrm{P}(S_1 = s_1)$, for $s_1 \in \mathscr{S}$, obtained through the procedure just described, depend heavily on the mix of LOS and NLOS scenarios and the inter-device distances we used in our data collection campaign. One is then faced with the question of whether our data collection campaign was representative of the "real-world". Another way of looking at the problem is that the right hand side of Eq. (14) is the sum of $2N$ terms, each being the natural logarithm of a probability. Hence, it may not matter what value we use for one of these terms. Hence, it may be acceptable to drop the first term from the cost function. Another possibility is to assume that $\mathrm{P}(S_1 = s_1) = 1/(2J)$, for any $s_1 \in \mathscr{S}$, which would again allow us to drop the first term from the cost function.

Next we turn our attention to the second term in the right hand side of Eq. (14). In order to estimate $\mathrm{P}(P_{R,j} = p_{R,j}|S_j = s_j)$, we construct a histogram of RSSI values of all data records labeled s_j. The histogram may be zero for certain values of $p_{R,j}$. (We know that for a BLE device, RSSI values range from about -40 to -100 or -120 dBm depending on receiver sensitivity.) To alleviate this problem, once again we use a smooth curve fitting approach, sample that curve at each integer in the possible RSSI range, and normalize the histogram so that its terms add up to one.

The third term in the right hand side of Eq. (14) is the hardest to handle. It requires some knowledge of how humans move and the "density" of walls in an indoor environment. The latter could be measured by how many walls on the average a straight line segment of a fixed length, say 10 m, would intersect. For example, ignoring blockage by other people, any pair of individuals would always be in LOS of each other in a soccer field or a large hotel ballroom. On the other hand, they would be in a NLOS situation most of the time in a building with lots of small rooms. The devices carried by the two individuals have no way of determining what type of environment they are in from a wall density point of view. Therefore, we do not model that aspect. As for a human mobility model, we assume that each individual can move at any speed from zero up to 1.4 m/s, which corresponds to 5 Km/h, which is the average human walking speed.

Our task is to specify $P(S_j = s_j|S_{j-1} = s_{j-1})$ based on a reasonable model. In what follows, we use $P_{l,k}$ to denote this conditional probability if $S_{j-1} = k$ and $S_j = l$, with $k,l \in \{1,2,\ldots,2J\}$. If the distance between the two individuals is R_{j-1} at t_{j-1}, then their distance at t_j cannot be larger than $R_{j-1} + \beta$ or smaller than $\max(R_{j-1} - \beta, 0)$, where $\beta = 2.8\Delta_j$. Let w be an adjustable positive system parameter. We propose the model given below:

$$
\begin{aligned}
\theta \triangleq P_{k,k} &= \frac{(2J-1)e^{-w\Delta_j}+1}{2J} \quad ; \quad \text{for } 1 \le k \le 2J \\
P_{l,k} &= \begin{cases}
c_k \max(\beta - (\eta_{l-1} - \eta_k), 0) & ; \quad \text{for } 1 \le k < l \le J \\
c_k \max(\beta - (\eta_{k-1} - \eta_l), 0) & ; \quad \text{for } 1 \le l < k \le J \\
c_k \beta & ; \quad \text{for } 1 \le k \le J \text{ and } l = k+J \\
c_k \max(\beta - (\eta_{l-J-1} - \eta_k), 0) & ; \quad \text{for } 1 \le k < l-J \le J \\
c_k \max(\beta - (\eta_{k-1} - \eta_{l-J}), 0) & ; \quad \text{for } 1 \le l-J < k \le J \\
c_{k-J} \max(\beta - (\eta_{l-J-1} - \eta_{k-J}), 0) & ; \quad \text{for } 1 \le k-J < l-J \le J \\
c_{k-J} \max(\beta - (\eta_{k-J-1} - \eta_{l-J}), 0) & ; \quad \text{for } 1 \le l-J < k-J \le J \\
c_{k-J} \beta & ; \quad \text{for } 1 \le k-J \le J \text{ and } l = k-J \\
c_{k-J} \max(\beta - (\eta_{l-1} - \eta_{k-J}), 0) & ; \quad \text{for } 1 \le k-J < l \le J \\
c_{k-J} \max(\beta - (\eta_{k-J-1} - \eta_l), 0) & ; \quad \text{for } 1 \le l < k-J \le J
\end{cases}
\end{aligned}
$$

where for $1 \le k \le J$,

$$c_k = (1-\theta)/D_k$$

and

$$D_k = \beta + 2\sum_{l=k+1}^{J} \max(\beta - (\eta_{l-1} - \eta_k), 0) + 2\sum_{l=1}^{k-1} \max(\beta - (\eta_{k-1} - \eta_l), 0)$$

Note that the first sum would be zero if $k = J$ and the second sum would be zero if $k = 1$.

The system of transition probabilities introduced above has two properties that one would expect in real-life. First,

$$\lim_{\Delta_j \to 0} \theta = 1$$

which implies the system state would remain the system when Δ_j tends to zero. This is expected because the distance between the individuals would not change when Δ_j tends to zero. Second, transitions to neighboring states are more likely than transitions to farther away states.

The state transitions described above exclude some, but not all, transitions that are physically impossible due to the 1.4 m/s speed limit. For example, consider the situation where two people are standing on the opposite sides of a wall at timestamp t_{j-1} and their distance is 1 m. If there is an opening in the wall, such as an open door, right next to where these people are standing, then it would be possible to have a transition to a state at timestamp t_j where these people are still 1 m apart but in LOS of each other. On the other hand, if these people are far from any such opening, then such a transition would not be possible. This suggests that state transitions depend on more than just the LOS/NLOS designation and how far apart a pair of people are.

We evaluated the performance of the mini-contact detection method proposed above using the data from all scenarios. We know that each LOS scenario with the distance between the devices less than or equal to 1.83 m is a situation with potential for virus transmission. There is no such potential in the remaining scenarios. Let's call these two types of scenarios I and II. For a given value of parameter w, a scenario of Type I contributes to the empirical calculation of $P_{\mathrm{D}}(w)$ only. We use a trellis with as many stages as the number of RSSI samples in the scenario. We then count the number of timestamps where the best path found by the VA goes through a state that belongs to $\mathscr{S}^*$. Similarly, a scenario of Type II contributes to the empirical calculation of $P_{\mathrm{FA}}(w)$ only. For each such scenario, once again we count the number of timestamps where the best path found by the VA goes through a state that belongs to $\mathscr{S}^*$.

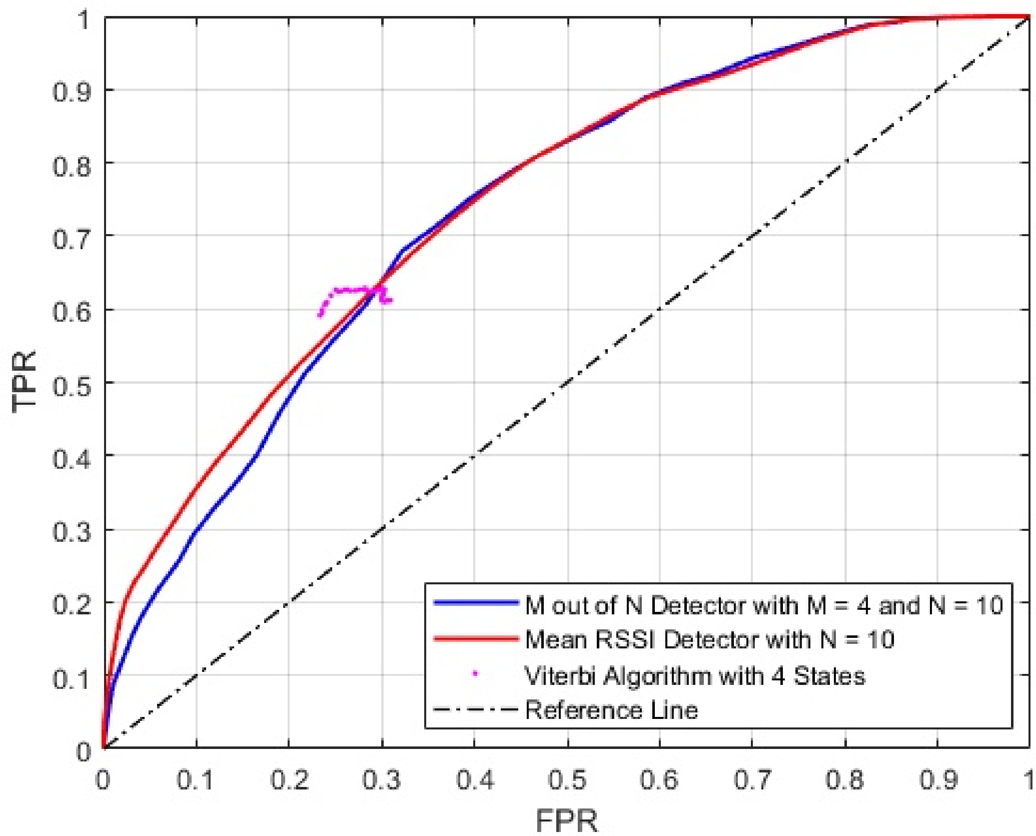

Fig. 14. ROC curves for VA-based mini-contact detection with $J = 2$ compared with other detectors

We evaluated the performance of the above systems with $J = 2$ and $J = 4$. The first case is straightforward, as $\eta_1 = 1.83$ m is the only threshold that defines the system states. For the $J = 4$ case, we used $\eta_1 = 1$ m, $\eta_2 = 1.83$ m, and $\eta_3 = 4.4$ m. One can argue that the values chosen for these thresholds are reasonable, but we made no attempt to optimize these choices. For each of the two systems, we let w vary from 0.1 to 3.0 with a step size of 0.1. That is, we tried 30 values of w for each system. For each value of w, a point in the ROC curve is obtained. The ROC curves for the systems with $J = 2$ and $J = 4$ are shown in Fig. 14 and Fig. 15, respectively. Also shown in each figure are the ROC curves for the best mean RSSI and M out of N detectors we have found. The first observation is that VA-based mini-contact detection can be modestly superior to the other two detectors, because for certain values of w one gets points that are above the ROC curves for the other two detectors. The second observation is that one can get better results with $J = 2$ than with $J = 4$. For example at $P_{\mathrm{FA}}(w) = 0.25$, one would get $P_{\mathrm{D}}(w) = 0.63$ with $J = 2$ and $P_{\mathrm{D}}(w) = 0.57$ with $J = 4$. This result may sound counter-intuitive, but it all depends on the system of transition probabilities we used and the RSSI thresholds that define system states.

While the ROC curves for the mean RSSI and M out of N detectors cover the full range of values $[0,1]$ for P_{FA} and P_{D}, the ROC curve for the VA-based approach has points in the intermediate range of values in the middle of the plot. The reason for this phenomenon is that we have imposed the condition that $\eta_{J^*} = 1.83$ m. If we had $\eta_1 = 100$ m, then we would get $P_{\text{FA}} = P_{\text{D}} = 1$, i.e. the northeast extreme point in the $P_{\text{FA}}P_{\text{D}}$-plane. On the other hand, if we had chosen $\eta_{J-1} = 0.1$ m, then we might get $P_{\text{FA}} = P_{\text{D}} = 0$, i.e. the southwest extreme point in the $P_{\text{FA}}P_{\text{D}}$-plane.

One advantage of the VA-based mini-contact detection is that it can handle scenarios with mobility. We did not look at such scenarios in this paper, because measuring the ground truth distance between two people that are moving around is quite challenging. In such scenarios, the two people involved get in and out of the situation where there is potential for virus transmission. The VA-based approach does inherently have the potential to estimate the time instances where such transitions take place. In contrast, the mean RSSI or the M out of N detector are better suited to scenarios without mobility, such as the two devices being stationary, e.g. when they are mounted on two tripods. All the BLE RSSI data we collected came from devices mounted on stationary tripods.

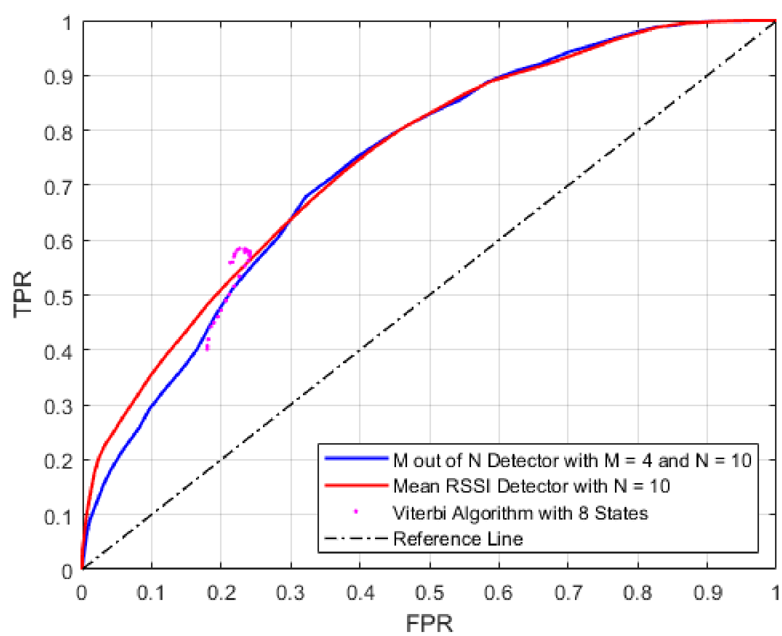

Fig. 15. ROC curves for VA-based mini-contact detection with $J = 4$ compared with other detectors

7. Related Work

Proximity detection is useful in many applications, and its history dates back to well before the recent focus on electronic contact tracing. In an early effort, GPS and mobile phone networks were proposed for proximity detection in the context of social networks [18]. The privacy aspects in this application was studied in Ref. [19]. Proximity detection with the aid of audio or light signals was developed in Ref. [20] to improve the security of NFC transactions. Proximity detection and alert technology was proposed for use at construction sites to reduce the number of fatalities resulting from workers being struck by an object or piece of construction equipment [21]. There are many use cases for proximity detection in the Internet of Things (IoT). The problems with the use of passive RFID tags in this context was studied in Ref. [22], where a solution based on a new RFID device was proposed. In certain IoT applications, close physical proximity can be used as a basis for trust. While some solutions rely on the use of multiple antennas for this purpose, a solution using a single antenna was proposed in Ref. [23]. Yet another paper studies integration of GPS and wireless communications for proximity detection in the context of wildlife monitoring [24]. Reference [25] argues that proximity detection based on technologies such as 802.15.4, BLE, and RFID fall short on metrics such as boundary sharpness, robustness against interference, and obstacle penetration. It proposes a method based on magnetic induction and evaluates it in a large food court to offer context-aware and personalized advertisements and diet suggestions at a per-counter granularity level. Relevant to our work, a number of papers have investigated the use of BLE/Bluetooth for proximity detection. The BlueEye system, developed in Ref. [26], uses Bluetooth received signal strength and relative orientation of mobile phones to gauge the extent of social interactions between people at large gatherings. Proximity detection can be used "to detect and distinguish interactions in the workplace" and how it "can shed light over productivity, team work and on employees' use of space" [27]. They have developed a solution based on BLE technology and evaluated it in a commercial organization with 25 participants. Reference [28] studies BLE-based proximity detection in a dense concentration of users. It proposes a BLE scanning mechanism that adapts itself to the user density to achieve more accurate proximity detection.

Since the onset of COVID-19 in late 2019, many researchers have worked on developing electronic contact tracing. Some have worked on the proximity detection aspect. Some have looked at the privacy aspect. There have also been several papers on evaluating how well proximity detection based on the BLE RSSI works. A comprehensive two-part survey of social distancing for preventing the spread of viral diseases such as COVID-19 can be found in Refs. [29, 30]. Part I provides the basics of social distancing, measurements, models, and it proposes practical usage scenarios with a focus on wireless technologies. Part II deals with other emerging technologies, such as machine learning, computer vision, thermal, and ultrasound, as they apply to social distancing. It also discusses privacy, scheduling, and incentive mechanisms in implementations of social distancing in practice. A survey of COVID-19 contact tracing apps is presented in Ref. [31]. Another survey paper focuses on using BLE for automatic contact tracing [32].

One has to be concerned about neighbor discovery before worrying about proximity detection. When a large number of smartphones or wearable devices are in the vicinity of each other, for example as in the case of students in a classroom, there is no guarantee that every device would "see" all others, i.e. sense their presence. Neighbor discovery is studied in Ref. [33]. The paper looks at the Bluetooth Specifications, limitations imposed by Android OS and iOS, and GAEN specifications. It uses the maximum time it takes to discover a neighbor as the performance metric as well as energy consumption. The paper concludes that neighbor discovery within reasonable time and without depleting battery power quickly is possible with a wearable device. It states that contact-tracing smartphone apps rely heavily on GAEN and can reliably detect only those contacts whose durations are at least five minutes long. Reference [34] presents a stochastic simulation modeling of contact tracing as a key control measure in the battle against infectious diseases when dealing with low numbers of cases. It presents a simple relationship between the efficiency of contact tracing necessary for eradication of an infectious disease and the basic reproductive ratio of the disease. A qualitative discussion of the factors that affect the effectiveness of a digital contact tracing wearable device is presented in Ref. [35]. These include distance estimation accuracy, energy consumption, and privacy preservation. The paper also provides a brief overview of existing solutions.

It is not feasible to assess the performance of proximity detection techniques without data collection, such as the one that was carried out in support of this paper. Just as in any ML/AI application, collecting annotated data for proximity detection in the context of electronic contact tracing is expensive. There have been a number of data collection campaigns and pilot studies around the world. Most of the data resulting from these efforts were collected in LOS scenarios, as it is considerably harder to measure the ground truth distance between a pair of devices used for proximity detection in NLOS scenarios than in LOS ones. MIT PACT [36] was a collaboration between academia, industry, government agencies, and other stakeholders led by MIT and a few partners. Its mission was "to enhance contact tracing in pandemic response by designing exposure detection functions in personal digital communication devices that have maximal public health utility while preserving privacy." The BLE RSSI data collected within PACT and a number of their technical reports can be found at the PACT website [36]. Some of the data collected came from scenarios where the smartphone(s) used for data collection were in a person's front or back pocket. The US National Institute of Standards and Technology (NIST), in coordination with the MIT PACT, organized and ran the Too Close for Too Long (TC4TL) Challenge [37]. The objectives of the Challenge were to (i) explore promising new ideas in TC4TL detection using BLE signal, (ii) support the development of advanced technologies incorporating these ideas, and (iii) measure performance of the state-of-the-art TC4TL detectors. There was another effort at NIST [38] similar to the work presented in this paper. Wearable devices based on the Silicon Labs Thunderboard (SLTB010A EFR32BG22 Thunderboard Kit) were developed and handed to seventeen participants to collect BLE RSSI data in 10 households. A web interface was used for participants to log and annotate the collected data after uploading it from the device via a Bluetooth connection. The performance of the M out of N detector was evaluated on the collected data. Reference [39] presented measurements taken on mobile handsets at approximately 1 Hz rate using two pairs of Android phones in four real-world scenarios: people walking outdoors in city streets, people sitting around a meeting table, people sitting in a train carriage and people grocery shopping in a supermarket. They measured the effect on received signal strength caused by the human body, by different types of indoor walls, the relative orientation of mobile handsets and so on. Based on the classical approach presented in Subsec. 4.1, the paper concluded that proximity detection based on BLE RSSI is hard and that apps based on BLE are therefore probably not a panacea but rather are best viewed as a potentially useful addition to existing contact tracing methods. They suggested that ML techniques may do better, but they acknowledged that it requires collecting a lot of annotated data. Reference [40] presents the results of a small-scale, 11-day pilot study to evaluate the performance of the TraceTogether app, the first Bluetooth-based contact tracing app, in the National Centre for Infectious Diseases (NCID) in Singapore in May 2020. The app was not able to record a contact between an iPhone and an Android phone. The contacts recorded by the app was compared to those recorded by a Real-Time Locating System (RTLS). The gold standard for contacts, however, was the patients' electronic medical records (EMR). It was shown that the RTLS detected 95.3% of the contacts, but TRaceTogether detected only 6.5%. Results on COVID-19 risk assessment based on extensive measurements of BLI RSSI in controlled synthetic and semi-controlled real-world experiments were presented in Ref. [41]. Similar to GAEN, the risk is computed as a linear combination of total periods of time in 24 hours a person is near, at an intermediate distance, far away, and very far away from an infected person. These four categories are decided by signal attenuation or equivalently RSSI ranges. The paper optimized the parameters of this model and showed how well the system worked under a large number of scenarios. The paper also has measurement results on signal attenuation as it goes through different types of materials and for various combinations of orientation for two BLE smartphones. The paper showed that optimized parameters vary from one application to another. Compromises have to be made between energy costs, applicability, accuracy, and reliability.

Machine learning (ML) can potentially help with proximity detection, which after all is a classification problem. A number of researchers have applied ML techniques to proximity detection in the context of COVID-19. ML provides a natural way of using measurements from other sensors in addition to BLE RSSI to do a better job of proximity detection. For example, the accelerometer, gyroscope, and magnetometer may help with estimating the relative orientations of two devices with respect to each other. Similarly, a light sensor may help with determining whether a device is in a pocket/purse or not. These in turn can help with how one interprets RSSI measurements and infer proximity from it. Reference [42] proposed Proximity-Based Privacy-Preserving Contact Tracing (P3CT) which was developed for use with a smartwatch and BLE RSSI. The use of a smartwatch reduces NLOS cases compared to the use of a smartphone, because a smartphone may be in a pocket or a purse. They use four different ML and classification techniques to classify the exposure risk of a user. A unique feature of the paper is the use of ambient signatures to anonymize the infected person's identity. This is the set of BLE RSSIs the person's smartwatch measures at any time. They collected their own data, which amounted to 37,644 BLE RSSI data points. They showed that a decision tree approach performs well in detecting proximity and assessing risk in the sense of high precision, recall, F1-score, and accuracy. They measured not just proximity, but also the time duration of two users being in close proximity, which we call a mini-contact in this paper. A pair of papers [12, 43] by another research group investigated ML techniques applied to BLE RSSI data collected by smartphones. They compared proximity detection performance of classical estimation techniques of Sec. 4 with those of three ML algorithms, namely, Support Vector Machines, Random Forest, and Gradient Boosted Machines. They showed that ML techniques achieved 3.60-19.98% better precision than the classical approach. In their second paper [43], they applied 19 ML classification and regression methods to not just BLE RSSI data, but also accelerometer and gyroscope data available on smartphones. Their model outperformed the state-of-the-art methods using neural networks and achieved a Normalized Decision Cost Function (nDCF) score of 0.34 with Bluetooth radio and 0.36 with sensor fusion. The use of Wi-Fi signal and ML techniques for contact tracing was explored in Ref. [44]. Their method uses Wi-Fi signal data to decide if two people shared the same physical space. Simulation results show up to 95% tracing accuracy depending on area size. It was argued in Ref. [45] that (i) COVID-19 virus transmission is a much bigger issue indoors than outdoors, (ii) people spend about 80% of their time indoors, and (iii) public places, where people are more likely to get infected by the virus, have a good density of Wi-Fi access points. The paper proposed ML-based methods for deciding whether Wi-Fi fingerprints collected by two agents come from devices that are within 2 m of each other or not. They showed that a single binary classifier will not do well, but an ensemble of three classifiers for environments with low, medium, and high density of Wi-Fi access points could yield 70% balanced accuracy on the average.

8. Conclusions

In the course of this research we carried out a comprehensive BLE RSSI data collection campaign, the likes of which are hard to find anywhere else, particularly when it comes to annotated NLOS data. We evaluated the performance of a few distance estimation methods based on the classical power law path loss model for RF signal propagation fitted to our collected data. We looked at the notion of confidence [12] as a way of evaluating proximity detection performance. Alternatively, we used the ROC curve for characterizing the performance of mean RSSI and M out of N proximity detection methods. We introduced the notions of instantaneous and after the fact proximity detection. We called the latter mini-contact detection and used the Viterbi Algorithm to solve the problem.

The ROC curves for various methods are not impressive because they are not significantly above the $P_{\mathrm{D}} = P_{\mathrm{FA}}$ line. One can get performance corresponding to any point (p, p) on that line by simply flipping an unfair coin with probability p for heads and deciding the H_1 hypothesis is true if one gets a heads. This approach does not even need any BLE RSSI data! One can get better performance by using ML techniques particularly when other sensors are available on the wearable devices. However, use of other sensors such as accelerometer and gyroscope comes at the expense of depleting the device battery much faster.

It is known that COVID-19 virus transmission depends on many factors and not just the distance between two people and whether there is a barrier between them. These other factors include ventilation and air flow, the relative orientation of the the two individuals, whether they are talking or eating, when one is sitting or lying down on the floor and the other standing, etc. Automatic detection of these other factors requires the availability of other sensors on proximity detection devices. We know that the US CDC changed its criteria for when the COVID-19 virus may get transmitted from one person to another a few times. There is also the question of whether the virus gets transmitted via droplets only or it is airborne. It is safe to say that it is not completely understood how the virus gets transmitted. However, this should not stop of us from trying to do proximity detection as accurately as possible. It has other applications also.

Ranging based on ultra-wideband RF signals or ultrasound [46, 47] are promising approaches that should be pursued. While ranging based on BLE RSSI has errors that can be measured in meters, UWB systems can easily achieve ranging error as low as 10-20 cm. Ultrasound is even better and one can achieve around 5 cm ranging error with inexpensive parts (buzzer and microphone). UWB has the advantage of being available on the latest iPhones and some Android phones. The challenge with UWB is that its signals propagates through certain types of walls. Therefore, two people less than 1.83 m apart but on opposite sides of a wall may cause the wearable device or smartphone to think that it is in a situation with potential for virus transmission. Ultrasound does not have this problem, but it suffers from another problem. Buzzers and microphones are directional. They can provide accurate ranging if the devices are facing each other, but the devices may not see each other or the range estimate might be way off if the devices are at an angle with respect to each other. Hence, there are challenges that have to be solved before UWB or ultrasound can work well for proximity detection in the context of electronic contact tracing.

Neighbor discovery is an important issue that deserves to be studied. There is no guarantee that the device worn by a student or the student's smartphone would see the devices/smartphones of all other students in a classroom when the Bluetooth specification of GAEN protocols is used for neighbor discovery.

References

[1] Boylston A (2014) John Haygarth's 18th-century 'rules of prevention' for eradicating smallpox. *Journal of the Royal Society of Medicine* 107(12):494–499.

[2] New York Times article (2020) N.Y.C. hired 3,000 workers for contact tracing. It's off to a slow start. (June 21, 2020). Available at https://www.nytimes.com/2020/06/21/nyregion/nyc-contact-tracing.html.

[3] CDC Guidance (2021) Operational considerations for adapting a contact tracing program to respond to the COVID-19 pandemic in non-US settings. Available at https://www.cdc.gov/coronavirus/2019-ncov/global-covid-19/operational-considerations-contact-tracing.html#:~:text=Close%20contact%20is%20defined%20by,by%20local%20risk%20assessments.

[4] GAEN Specifications (2020) Exposure notifications: Using technology to help public health authorities fight COVID 19. Available at https://www.google.com/covid19/exposurenotifications/.

[5] Adoption Rate Statistics (2021) Here are the countries using Google and Apple's COVID-19 Contact Tracing API. Available at https://www.xda-developers.com/google-apple-covid-19-contact-tracing-exposure-notifications-api-app-list-countries/.

[6] Pew Research Center article (2019) Smartphone ownership is growing rapidly around the world, but not always equally. (Feb. 5, 2019). Available at https://www.pewresearch.org/global/2019/02/05/smartphone-ownership-is-growing-rapidly-around-the-world-but-not-always-equally/.

[7] Pew Research Center article (2020) The challenges of contact tracing as U.S. battles COVID-19. (Oct. 30, 2020). Available at https://www.pewresearch.org/internet/2020/10/30/the-challenges-of-contact-tracing-as-u-s-battles-covid-19/.

[8] Forbes Magazine article (2019) More seniors are embracing technology. But can they use it? UCSD researchers suggest asking them. (June 28, 2019). Available at https://www.forbes.com/sites/robinseatonjefferson/2019/06/28/more-seniors-are-embracing-technology-but-can-they-use-it-ucsd-researchers-suggest-asking-them/?sh=7412d0fc2323.

[9] Panda Security article: When should kids get smartphones? (Survey). Available at https://www.pandasecurity.com/en/mediacenter/panda-security/when-should-kids-get-smartphones/.

[10] Moayeri N (2022) Bluetooth Low Energy (BLE) Received Signal Strength Indicator (RSSI) Data for Proximity Detection in COVID-19 Electronic Contact Tracing. Available at https://doi.org/10.18434/mds2-2827.

[11] Rappaport T (2002) *Wireless Communications: Principles and Practice* (Prentice Hall), 2nd Ed.

[12] Su Z, Pahlavan K, Agu E (2021) Performance evaluation of covid-19 proximity detection using bluetooth le signal. *IEEE Access* 9.

[13] Dinneen G, Reed I (1956) An analysis of signal detection and location by digital methods. *IRE Transactions on Information Theory* 2(1):29–38.

[14] Schwartz M (1956) A coincidence procedure for signal detection. *IRE Transactions on Information Theory* 2(4):135–139.
[15] Mrstik A (1978) Multistatic-radar binomial detection. *IEEE Transactions on Aerospace and Electronic Systems* 14(1):103–108.
[16] Norouzi Y, Greco M, Nayebi M (2006) Performance evaluation of k out of n detector. *14th European Signal Processing Conference* :1–5.
[17] Forney G (1973) The viterbi algorithm. *Proceedings of the IEEE* 61:268–278.
[18] Amir A, Efrat A, Myllymaki J, Palaniappan L, Wampler K (2007) Buddy tracking — efficient proximity detection among mobile friends. *Pervasive and Mobile Computing* 3(5):489–511.
[19] Šikšnys L, Thomsen J, Šaltenis S, Yiu M (2010) Private and flexible proximity detection in mobile social networks. *Proceedings of the Eleventh International Conference on Mobile Data Management* :75–84.
[20] Halevi D, Ma D, Saxena N, Xiang T (2012) Secure proximity detection for nfc devices based on ambient sensor data. *Proceedings of the European Symposium on Research in Computer Science* :379–396.
[21] Marks E, Teizer J (2013) Method for testing proximity detection and alert technology for safe construction equipment operation. *Construction Management and Economics* 6 Occupational Health and Safety in the Construction Industry:636–646.
[22] Bolic M, Rostamian M, Djuric P (2015) Proximity detection with rfid: A step toward the internet of things. *IEEE Pervasive Computing* 14(2):70–76.
[23] Pierson T, Peters T, Peterson R, Kotz D (2019) Proximity detection with single-antenna iot devices. *MobiCom '19: The 25th Annual International Conference on Mobile Computing and Networking* :1–15.
[24] Picco G, Molteni D, Murphy A, Ossi F, Cagnacci F, Corrà M, Nicoloso S (2015) Geo-referenced proximity detection of wildlife with WildScope: design and characterization. *IPSN '15: Proceedings of the 14th International Conference on Information Processing in Sensor Networks* :238–249.
[25] Jiang X, Liang CJM, Chen K, Zhang B, Hsu J, Liu J, Cao B, Zhao F (2012) Design and evaluation of a wireless magnetic-based proximity detection platform for indoor applications. *IPSN '12: Proceedings of the 11th international conference on Information Processing in Sensor Networks* :221–232.
[26] Ghose A, Bhaumik C, Chakravarty T (2013) BlueEye: a system for proximity detection using Bluetooth on mobile phones. *UbiComp '13 Adjunct: Proceedings of the 2013 ACM Conference on Pervasive and Ubiquitous Computing* :1135–1142.
[27] Montanari A, Nawaz S, Mascolo C, Sailer K (2017) A study of Bluetooth Low Energy performance for human proximity detection in the workplace. *2017 IEEE International Conference on Pervasive Computing and Communications (PerCom)* :1–10.
[28] Ng P, She J, Park S (2018) High resolution beacon-based proximity detection for dense deployment. *IEEE Transactions on Mobile Computing* 17(6):1369–1382.
[29] Nguyen C, Saputra Y, Huynh N, Nguyen NT, Khoa T, Tuan B, Nguyen D, Hoang D, Vu T, Dutkiewicz E, Chatzinotas S, Ottersten B (2020) A comprehensive survey of

enabling and emerging technologies for social distancing - Part I: Fundamentals and enabling technologies. *IEEE Access* 8:153479–153507.

[30] Nguyen C, Saputra Y, Huynh N, Nguyen NT, Khoa T, Tuan B, Nguyen D, Hoang D, Vu T, Dutkiewicz E, Chatzinotas S, Ottersten B (2020) A comprehensive survey of enabling and emerging technologies for social distancing - Part II: Emerging technologies and open issues. *IEEE Access* 8:154209–154236.

[31] Ahmed N, Michelin R, Xue W, Ruj S, Malaney R, Kanhere S, Seneviratne A, Hu W, Janicke H, Jha S (2020) A survey of covid-19 contact tracing apps. *IEEE Access* 8:134577–134601.

[32] Reichert L, Brack S, Scheuermann B (2021) A survey of automatic contact tracing approaches using bluetooth low energy. *ACM Transactions on Computing for Healthcare* 2(2):1–33.

[33] Kindt P, Chakraborty T, Chakraborty S (2022) How reliable is smartphone-based electronic contact tracing for covid-19? *Communications of the ACM* 65(1):56–67.

[34] Eames K, Keeling M (2003) Contact tracing and disease control. *Proceedings of Royal Society B* 270(1533):2565–2571.

[35] Shubina V, Ometov A, Lohan E (2020) Technical perspectives of contact-tracing applications on wearables for covid-19 control. *12th International Congress on Ultra Modern Telecommunications and Control Systems and Workshops (ICUMT)* :229–235.

[36] MIT PACT Consortium (2020) Private automated contact tracing Available at https://pact.mit.edu/.

[37] NIST Too Close for Too Long (TC4TL) Challenge (2020) Available at https://www.nist.gov/itl/iad/mig/nist-tc4tl-challenge.

[38] Keenan K, Aumentado J, Booth H, Briggman K, Kraft M, Martin M, Peralta R, Robinson A, Shalm K, Stephens M, Townsend E, Nam S (2021) Development and evaluation of bluetooth low-energy device for electronic encounter metrics. *Journal of Research of the National Institute of Standards and Technology* 126:1–19.

[39] Leith D, Farrell S (2020) Coronavirus contact tracing: evaluating the potential of using bluetooth received signal strength for proximity detection. *ACM SIGCOMM Computer Communication Review* 50(4):66–74.

[40] Huang Z, Guo H, Lee YM, Ho E, Ang H, Chow A (2020) Performance of digital contact tracing tools for covid-19 response in Singapore: Cross-sectional study. *JMIR MHEALTH AND UHEALTH* 8(10):1–10.

[41] Meyer S, Windisch T, Perl A, Dzibela D, Marzilger R, Witt N, Benzler J, Kirchner G, Feigl T, Mutschler C (2021) Contact tracing with the exposure notification framework in the german corona-warn-app. *The 11th International Conference on Indoor Positioning and Indoor Navigation (IPIN)* :1–8.

[42] Ng P, Spachos P, Gregori S, Plataniotis K (2022) Epidemic exposure tracking with wearables: A machine learning approach to contact tracing. *IEEE Access* 10:14134–14148.

[43] Semenov O, Agu E, Pahlavan K, Su Z (2022) Covid-19 social distance proximity

estimation using machine learning analyses of smartphone sensor data. *IEEE Sensors Journal* 22(10):9568–9579.

[44] Narzullaev A, Muminov Z, Narzullaev M (2020) Contact tracing of infectious diseases using wi-fi signals and machine learning classification. *IEEE 2nd International Conference on Artificial Intelligence in Engineering and Technology (IICAIET)* :1–5.

[45] Hyfte ZV, Zakhor A (2021) Immediate proximity detection using wi-fi–enabled smartphones. *The 11th International Conference on Indoor Positioning and Indoor Navigation (IPIN)* :1–8.

[46] Qorvo Products Use Case (2020) Ultra-wideband and contact tracing 101 Available at https://www.qorvo.com/design-hub/blog/ultra-wideband-and-contact-tracing.

[47] Meklenburg J, Specter M, Wentz M, Balakrishnan H, Chandrakasan A, Cohn J, Hatke G, Ivers L, Rivest R, Sussman G, Weitzner D (2020) SonicPACT: An ultrasonic ranging method for the private automated contact tracing (PACT) protocol Available at https://pact.mit.edu/wp-content/uploads/2020/11/SonicPACT_Final_v2-with-logos-revA.pdf.

Appendix A. BLE RSSI Data Collection Scenarios

The following factors and possible choices for them apply to all scenarios:

- Each device was at a height of 120 cm from the ground/floor.
- Two combinations of orientations were used in each scenario, as shown in Fig. 16 and Fig. 17. In the combination shown in Fig. 16, the two devices were facing each other. In the combination shown in Fig. 17, the two devices were facing up. In what follows, we call the orientation in Fig. 16 as Orientation 1 and the other as Orientation 2.

Fig. 16. Possible combinations of orientations for a pair of devices: Two devices facing each other

Fig. 17. Possible combinations of orientations for a pair of devices: Two devices facing up

The following factors and possible choices for them apply to all LOS scenarios with Orientation 1:

- Up to three choices of a person being on the direct path, with the caveat that it would not be possible for a person to be between the devices if they are too close to each other:
  - No one on the direct path
  - Person @ 0.5 m from Device 1
  - Person @ the midpoint of the horizontal line connecting the devices

Note that for Orientation 2, we tested only without anybody on the direct path.

Appendix A.1. LOS Scenarios

LOS Scenario 1: Narrow Corridor

- Bldg. 222, 2nd Floor, Corridor B
- Horizontal distance between devices placed along the corridor: 0.5 m, 1.0 m, 1.5 m, 2.0 m, 2.5 m, 3.0 m, 3.5 m, 4.0 m, 4.5 m, 5.0 m, 6.0 m, 7.0 m, 8.0 m, 9.0 m, 10 m, 12 m, 15 m, 20 m

LOS Scenario 2: Parking Lot

- Bldg. 222 parking lot
- Horizontal distance between devices: 0.5 m, 1.0 m, 1.5 m, 2.0 m, 2.5 m, 3.0 m, 3.5 m, 4.0 m, 4.5 m, 5.0 m, 6.0 m, 7.0 m, 8.0 m, 9.0 m, 10 m, 12 m, 15 m, 20 m

LOS Scenario 3: Wide Corridor

- Bldg. 101, 1st Floor, The old Hall of Flags Corridor
- Horizontal distance between devices placed along the corridor: 0.5 m, 1.0 m, 1.5 m, 2.0 m, 2.5 m, 3.0 m, 3.5 m, 4.0 m, 4.5 m, 5.0 m, 6.0 m, 7.0 m, 8.0 m, 9.0 m, 10 m, 12 m, 15 m, 20 m

LOS Scenario 4: Small Office

- Bldg. 222, 2nd Floor, a single-module office belonging to ANTD (Division 772)
- Horizontal distance between devices along the length of office: 0.5 m, 1.0 m, 1.5 m, 2.0 m, 2.5 m, 3.0 m, 3.5 m, 4.0 m

LOS Scenario 5: Large Room with High Ceiling

- Bldg. 101 Cafeteria

- Horizontal distance between devices placed in the Cafeteria: 0.5 m, 1.0 m, 1.5 m, 2.0 m, 2.5 m, 3.0 m, 3.5 m, 4.0 m, 4.5 m, 5.0 m, 6.0 m, 7.0 m, 8.0 m, 9.0 m, 10 m, 12 m, 15 m, 20 m

LOS Scenario 6: Same Flight of a Stairwell

- Bldg. 222 East Stairwell
- The devices were placed on different steps of the same flight in the stairwell, i.e., the devices were at different heights. The distance between the devices were 0.88 m, 1.06 m, 1.5 m, 2.06 m, 2.66 m, or 3.28 m. In the 0.88 m case, no one was on the direct path. For other distances, we tested with “no one on the direct path” and a “person @ 0.5 m from Device 1”. In addition, we only used Orientation 1.
- Both devices were horizontally in the middle of the stairwell.

LOS Scenario 7: Opposite Flights in a Stairwell

- Bldg. 222 East Stairwell
- The devices were initially placed on the two flights horizontally across from each other. Then the two devices were moved by several steps in opposite directions, i.e., as if both people are walking down the stairs or both walking up.
- In this scenario, we only tested Orientation 1 with no one on the direct path.
- We tested six different combinations of positions. The distances between two devices were: 3.68 m, 2.85 m, 2.30 m, 2.23 m, 2.65 m and 3.39 m. We explain why these distances are not in increasing order. The data collection began when Person 1 and Person 2 were at Floors 1 and 0.5 in the stairwell, respectively. Data was collected. Then each person walked down a couple of stairs in the respective flights, and data was taken again, and so forth. Therefore, the distance between the devices would decrease first and reach its minimum when both persons get to the middle of their respective flights, and it would start increasing after that.
- Both devices were horizontally in the middle of the stairwell.

Appendix A.2. NLOS Scenarios

NLOS Scenario 1: Partitioned Office

- Plenty of such offices in Bldg. 222
- Two devices on opposite sides of a partition at the same distance from the partition
- Horizontal distance between devices: 0.5 m, 1.0 m, 1.5 m, 2.0 m, 2.5 m, 3.0 m, 3.5 m, 4 m

NLOS Scenario 2: One Wooden Door Separating the Devices

- Plenty of such doors in Bldg. 222
- Two devices on opposite sides of a wooden door at the same distance from the door
- Horizontal distance between devices: 0.5 m, 1.0 m, 1.5 m, 2.0 m, 2.5 m, 3.0 m, 3.5 m, 4 m

NLOS Scenario 3: One Glass Wall Separating the Devices

- Bldg. 301
- Two devices on opposite sides of a wall at the same distance from the wall
- Horizontal distance between devices: 0.5 m, 1.0 m, 1.5 m, 2.0 m, 2.5 m, 3.0 m, 3.5 m, 4 m

NLOS Scenario 4: One Cinder Block Wall Separating the Devices

- Bldg. 301
- Two devices on opposite sides of a wall at the same distance from the wall
- Horizontal distance between devices: 0.5 m, 1.0 m, 1.5 m, 2.0 m, 2.5 m, 3.0 m, 3.5 m, 4 m

NLOS Scenario 5: One Brick Block Wall Separating the Devices

- Plenty of such walls in Bldg. 301 or Basement of Building 101
- Two devices on opposite sides of a wall at the same distance from the wall
- Horizontal distance between devices: 1.0 m, 1.5 m, 2.0 m, 2.5 m, 3.0 m, 3.5 m, 4 m

NLOS Scenario 6: One Dry Wall Separating the Devices

- Plenty of such walls in Bldg. 222
- Two devices on opposite sides of a wall at the same distance from the wall
- Horizontal distance between devices: 0.5 m, 1.0 m, 1.5 m, 2.0 m, 2.5 m, 3.0 m, 3.5 m, 4 m

NLOS Scenario 7: One Granite Wall Separating the Devices

- Bldg. 101, close to the auditoriums
- Two devices on opposite sides of a wall at the same distance from the wall
- Horizontal distance between devices: 1.0 m, 1.5 m, 2.0 m, 2.5 m, 3.0 m, 3.5 m

NLOS Scenario 8: One Metal Wall Separating the Devices

- Plenty of such walls in Bldg. 222
- Two devices on opposite sides of a wall at the same distance from the wall

- Horizontal distance between devices: 0.5 m, 1.0 m, 1.5 m, 2.0 m, 2.5 m, 3.0 m, 3.5 m, 4 m

NLOS Scenario 9: Two Parallel Dry Walls Separating the Devices

- A number of such situation in Bldg. 222
- Horizontal distance from each device to the wall closest to it, with two walls between the devices: 20 cm, 40 cm, 60 cm, 80 cm, 100 cm, 140 cm, 180 cm, 200 cm
- The distances between the devices were 4.77 m, 5.27 m, 5.77 m, 6.27 m, 6.77 m, 7.27 m, 7.77 m, 8.27 m, respectively.

NLOS Scenario 10: Devices around a 90-Degree Corner Made of Two Cinder Block Walls

- Plenty of such corners in Bldg. 301
- Both devices at equal distances from the walls comprising the corner
- The distances between the devices were 1.41 m, 2.12m, 2.83 m, 3.54 m, 4.24 m, 2.83 m, 3.54 m, and 4.24 m. The positions of devices are shown in Fig. 18.

NLOS Scenario 11: Devices around a 90-Degree Corner Made of Two Dry Walls

- Several such corners in Bldg. 222
- Same settings as NLOS Scenario 10

NLOS Scenario 12: Devices around a 90-Degree Corner Made of Two Granite Walls

- Plenty of such walls in Bldg. 101, 1st Floor
- Same settings as NLOS Scenario 10

NLOS Scenario 13: Devices around a 90-Degree Corner Made of Two Metal Walls

- Several such corners in any General Purpose Laboratory (GPL) other than Bldg. 222
- Same settings as NLOS Scenario 10

NLOS Scenario 14: Different Floors

- Bldg. 222
- Device 1 was in Corridor B on the 1st floor. Device 2 was right above it on the 2nd or 3rd floors. We repeated the experiment at the following horizontal offsets from this initial placement for Device 2: 1.0 m, 2.0 m, 3.0 m, 4.0 m, 5.0 m, 6.0 m, 7.0 m, 8.0 m, 9.0 m, 10.0 m
- Hence, when Device 2 was on the 2nd floor, the distances between the devices were 3.55 m, 3.69 m, 4.08 m, 4.65 m, 5.35 m, 6.13 m, 6.97 m, 7.85 m, 8.75 m, 9.68 m, and 10.61 m. When Device 2 was on the 3rd floor, the distances between the devices

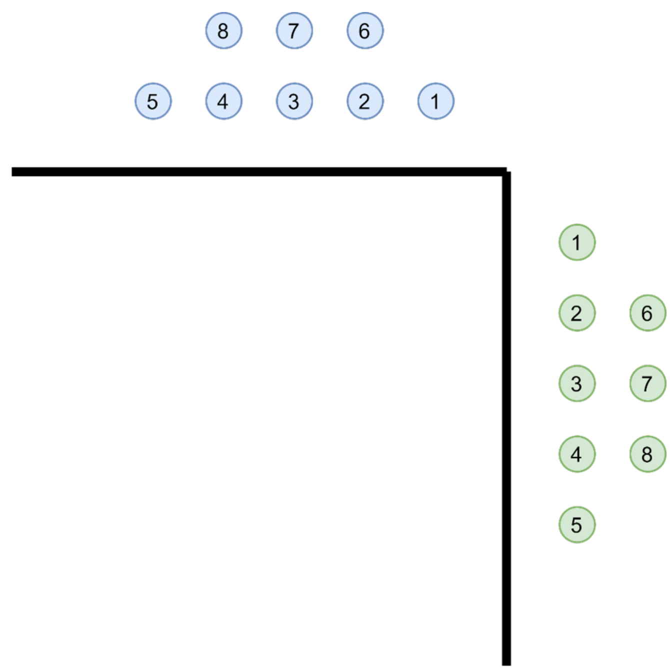

Fig. 18. Positions of the devices. The blue and green circles represent Device 1 and Device 2 positions, respectively. The number in each circle represents the index i for each test. That is, when Device 1 was at the position of Blue Circle i, Device 2 was at at the position of Green Circle i. For Tests 1 - 5, each device was 0.5 m away from the nearest wall. For Tests 6 - 8, each devices was 1 m away from the nearest wall. In addition, the distance between blue (green) circles 1 and 2, 2 and 3, . . . , 4 and 5, 6 and 7, 7 and 8 was 0.5 m.

were 7.09 m, 7.16 m, 7.37 m, 7.7 m, 8.14 m, 8.68 m, 9.29 m, 9.97 m, 10.69 m, 11.46 m, and 12.26 m.

NLOS Scenario 15: Half Floor in the Stairwell

- Bldg. 222
- We only used Orientation 1.
- One device was placed on the bottom of the stairwell, the other one at 0.5, 1, 1.5, 2, 2.5 and 3 floors higher than the first device. That is, the second device was placed at three half-floors in the stairwell as well as at 1, 2, or 3 floors higher right above the horizontal location of the first device.
- The distances between the devices were 4.65 m, 4 m, 7.04 m, 7.13 m, 9.9 m and 10.72 m, respectively.